Preequilibrium reactions with complex particle channels

C. Kalbach
Physics Department, Duke University, Durham, North Carolina 27708-0305
(Received 10 November 2004; published 22 March 2005)

Investigations of nucleon induced reactions at incident energies of 14–90 MeV resulting in the emission of complex particles ($A = 2$–4) have provided insights which complement those previously obtained from (N, xN) reactions. The description of the preequilibrium energy spectra required modifications to an earlier phenomenological model for direct pickup reactions. This model supplements the usual exciton preequilibrium model. Work on complex particle induced reactions confirms some of these results, extends them to include stripping and exchange reactions, and provides evidence for a projectile dependence of the average effective matrix elements for the residual interactions in the exciton model. A full description of reactions with complex projectiles will require the inclusion of a realistic breakup component and the resulting reduction of the cross section available for the exciton model calculations. Reactions with complex particles in the entrance and/or exit channels have provided indirect evidence for the amount of surface peaking of the initial target-projectile interaction. A summary of additional data needed to help resolve remaining questions is presented.

DOI: 10.1103/PhysRevC.71.034606 PACS number(s): 24.60.Gv, 24.10.Pa

I. INTRODUCTION

Early work on Griffin's exciton model [1] launched the field of preequilibrium reaction studies and led to the development of a whole host of models, both phenomenological (like the exciton model) and more quantum mechanical. These models describe the way in which the projectile energy gradually gets redistributed among the constituent nucleons of the composite system through a series of residual two-body interactions. They have been quite successful in reproducing both the energy spectra of emitted particles and the excitation functions for the formation of specific product nuclides in a wide range of reactions, but primarily for reactions involving only nucleons in the entrance and exit channels. Incident energies have typically ranged from 14 to 100 MeV, with a few papers (e.g., [2–4]) extending that range up to 200 MeV. These higher energies are important in applications such as the accelerator-driven transmutation of wastes.

Reactions which have light complex particles (deuterons, tritons, ^{3}He, and α particles) in the entrance and/or exit channels are more difficult to describe, having long been recognized to involve other reaction mechanisms such as direct nucleon transfer, knockout/inelastic processes involving cluster degrees of freedom, and projectile breakup. Various groups have modified the treatment of complex particles within the exciton model in attempts to account for experimental results without invoking other models, and there is continuing debate about the relative roles of, for instance, nucleon transfer and cluster knockout processes. This whole subject was recently summarized in a review article by Hodgson and Běták [5].

While significant progress has been made in the "exciton model only" approaches, particularly through the inclusion of a pickup mechanism that allows an emitted complex particle to "coalesce" from particles both above and below the Fermi level [6–8], they have yet to describe the wide variety of reactions treated in this paper. In addition, there are ad hoc assumptions and/or problems in deriving the modified complex particle emission rates from microscopic reversibility (see [9]). Finally, it appears to me that the physical picture is different from that of a direct nucleon transfer reaction, since the exciton model envisions a two-stage process—formation of a well defined composite state and subsequent emission—rather than the one-step direct transfer mechanism frequently invoked in spectroscopic studies. This work therefore assumes that the exciton model must be supplemented with models describing additional direct reaction mechanisms and presents progress toward a coherent and useful, though phenomenological, description of the complex particle reaction channels. The starting point is the two-component exciton model and some simple direct reaction models developed many years ago.

In previous work [10–12], the TUNL exciton model has been modified and benchmarked using comparisons with experimental energy spectra from inclusive (nucleon, nucleon) or (N, xN) reactions at energies of 14 to 25 MeV. At these lower energies, the data are more sensitive to pairing and shell structure effects. These issues, as well as the residual two-body matrix elements responsible for energy equilibration, have been studied and elucidated. Subsequent work on the amount of surface peaking of the initial target-projectile interaction in (N, xN) reactions [13] gave evidence that the model formulation works well up to incident energies of around 90 MeV. The need for additional work on the complex particle channels became evident when comparisons with data showed that changes in the exciton model state densities, which are used in the nucleon transfer model, actually worsened agreement with experiment in some cases. Other problems became apparent when more recent energy spectra from the literature were considered.

Initial studies were carried out with the database of angle-integrated energy spectra used in earlier work with a few additional spectra, and those interim results were included

 ©2005 The American Physical Society

in PRECO-2000 [14]. These spectra were later supplemented by additional readily accessible data, yielding a comprehensive but certainly not exhaustive database—one that provides broad coverage of projectiles, incident energies, and target masses. The present paper first describes results for reactions with incident nucleons, where the exciton model is already well benchmarked and where fairly definitive results could be obtained. Partial and preliminary (but hopefully still useful) results for complex particle induced reactions are also presented, particularly with regard to direct nucleon transfer reactions, where they serve to verify the work with incident neutrons and protons. It has become clear, however, that achieving an adequate and physically meaningful description of complex particle induced reactions will require careful consideration of projectile breakup and its impact on the remainder of the calculations.

Because the models describing complex particle channels are phenomenological, they involve a significant number of adjustable parameters. However, the variety of reactions for which the models must work is also quite large and places severe constraints on what can be done. Because of the breadth of the database, it is felt that the resulting descriptions will have significant predictive ability.

The next sections of this paper describe the status of the direct reaction models prior to this work, and the database used. Section IV discusses the work on nucleon induced complex particle emission, and Sec. V considers complex particle induced reactions. Section VI presents the resulting revised models; Sec. VII shows comparisons with many of the measured angle-integrated spectra; and Sec. VIII gives the summary and conclusions of this work.

II. SUMMARY OF EXISTING MODELS

This work uses the two-component exciton model formalism described in [10] as it was further developed in a series of papers [11–13,15]. This formalism, along with a few modifications from the present work, is summarized in the users' manual for PRECO-2000 [14]. The phenomenological models used to describe direct nucleon transfer processes and reactions involving cluster degrees of freedom were first developed in 1977 [16] and later modified for use in PRECO-D2 [17]. They are described below for the case where isospin is assumed to be fully mixed. The formalism in PRECO-2000 was the result of the first phase of this work.

A. Nucleon transfer

In the reaction $A(a,b)B$, the energy differential cross section for nucleon transfer (pickup, stripping, or nucleon exchange) is given by

$$\left[\frac{d\sigma_{a,b}(\varepsilon)}{d\varepsilon}\right]_{\mathrm{NT}} = \frac{2s_b+1}{2s_a+1}\,\frac{A_b}{A_a}\,\frac{\varepsilon\,\sigma_b(\varepsilon)}{A_a}\,K_{\alpha,p}\left(\frac{A_a}{E_a+V_a}\right)^{2n} \times \left(\frac{2860}{A_B}\right)^{n}\frac{1}{80\,\varepsilon_a}\sum_{p_\pi}\left(\frac{2Z_A}{A_A}\right)^{6n_\pi}\omega(p_\pi,h_\pi,p_\nu,h_\nu,U). \tag{1}$$

Here, N, Z, and A refer to the neutron, proton, and mass numbers of the nucleus designated by its subscript, and s is the spin of the designated particle. The energy variables are ε_a for the entrance channel energy, ε for the exit channel energy, and E_a for the projectile laboratory energy, while $\sigma_b(\varepsilon)$ gives the exit channel total nonelastic cross section. The quantities p_π, h_π, p_ν, and h_ν refer to the number of proton-particle, proton-hole, neutron-particle, and neutron-hole degrees of freedom in the residual nucleus and are determined by the number of stripped nucleons (for particles) or picked up nucleons (for holes). The quantity $n = p_\pi + h_\pi + p_\nu + h_\nu$ is the total number of excitons or degrees of freedom, and $n_\pi = p_\pi + h_\pi$ is the number of proton degrees of freedom. The quantity $\omega(p_\pi, h_\pi, p_\nu, h_\nu, U)$ is the density of the residual states at excitation energy U. When this formalism was developed, the state densities were evaluated in the simple equispacing model, without corrections for shell structure or the finite depth of the nuclear potential well. The sum over p_π is only used for inelastic reactions with weakly bound projectiles (d, t, or ^{3}He) where both proton and neutron exchange are allowed. The numerical constants are determined assuming that the energies are given in MeV and the cross sections are in mb. The constant $K_{\alpha,p}$ provides an enhancement factor of 12 for (N,α) and (α,N) reactions, where both projectile and ejectile are tightly bound. Finally, the quantity V_a is an empirical energy of (12.5 MeV) $\times$ A_a, which may represent the energy difference experienced by the projectile between infinity and the Fermi level of the nucleus. In any case, the factor $A_a/(E_a+V_a)$ seems to have the dimensions of $(\mathrm{velocity})^{-2}$.

Nucleon transfer is the primary mechanism needed to supplement the exciton model in nucleon induced reactions. Along with other mechanisms, it also plays a significant role for reactions with complex projectiles.

B. Reactions with cluster degrees of freedom

The reactions involving cluster degrees of freedom are assumed to occur when a complex projectile excites a neutron, proton, or α particle-hole pair while retaining its cluster identity or when a nucleon projectile excites an α particle-hole pair (nucleon pair excitation being considered in the exciton model). Each of these interactions forms a three-exciton, or two-particle–one-hole, state which decays by emission of one or the other particle degree of freedom. The relative intensities for these two types of emission are determined by phase space considerations. Thus, the energy differential cross sections for the knockout reaction $A(a,b)B$ are proportional to the entrance channel cross section and the appropriate phase space branching ratio. When the energy integrals in the denominator of the branching ratio are approximated in closed form, the cross section for knockout reactions takes on the form

$$\left[\frac{d\sigma_{a,b}(\varepsilon)}{d\varepsilon}\right]_{\rm KO} = C_{\rm CL}\,\sigma_a(\varepsilon_a)(2s_b+1)\,A_b\,\varepsilon\,\sigma_b(\varepsilon)\frac{\mathcal{P}_b\,g_a\,g_b\,[U-A_{\rm KO}(p_a,h_b)]}{\sum_{c=a,b}(2s_c+1)\,A_c\langle\sigma_c\rangle(\varepsilon_m+2B_{{\rm Coul},c})(\varepsilon_m-B_{{\rm Coul},c})^2 g_a\,g_b^2/6g_c}. \quad (2)$$

Similarly, for $A(a,a')A$ inelastic scattering where a is a complex particle, the cross section is

$$\left[\frac{d\sigma_{a,a'}(\varepsilon)}{d\varepsilon}\right]_{\rm IN} = C_{\rm CL}\sigma_a(\varepsilon_a)(2s_a+1)\,A_a\,\varepsilon\,\sigma_a(\varepsilon)\sum_{i=n,p,\alpha}\frac{\mathcal{P}_i\,g_i^2\,U}{\sum_{c=a,i}(2s_c+1)\,A_a\langle\sigma_c\rangle(\varepsilon_m+2B_{{\rm Coul},c})(\varepsilon_m-B_{{\rm Coul},c})^2 g_a\,g_i^2/6g_c}. \quad (3)$$

For nucleon inelastic scattering, the excitation of proton and neutron particle-hole pairs is already included in the exciton model so that only α pair excitation is included here, giving

$$\left[\frac{d\sigma_{a,a'}(\varepsilon)}{d\varepsilon}\right]_{\rm IN} = C_{\rm CL}\,\sigma_a(\varepsilon_a)(2s_a+1)\,A_a\varepsilon\,\sigma_a(\varepsilon)\frac{\mathcal{P}_\alpha\,g_\alpha^2\,U}{\sum_{c=a,\alpha}(2s_c+1)\,A_a\langle\sigma_c\rangle\,(\varepsilon_m+2B_{{\rm Coul},c})(\varepsilon_m-B_{{\rm Coul},c})^2 g_a g_\alpha^2/6g_c}. \quad (4)$$

In these equations, the overall normalization $C_{\rm CL}$ is the only adjustable parameter. (While the users' manual for PRECO-D2 quoted a normalization of $C_{\rm CL}=1/13.5$, what was actually found to be programmed was 1/16.) In these equations, $\mathcal{P}_i$ is the probability of exciting an i-type particle-hole pair, ε_m is the maximum emission energy in the c channel, and $B_{{\rm Coul},c}$ is the Coulomb barrier for a particle of type c. The quantity $\sigma_a(\varepsilon_a)$ is the entrance channel total reaction cross section, while $\langle\sigma_c\rangle$ is the inverse cross section in the c channel averaged over emission energies between $B_{{\rm Coul},c}$ and the maximum allowed. The factors of the type $g^2\,U$ give the final state density. The final state for knockout contains an a-type particle and a b-type hole. The Pauli correction function, $A_{\rm KO}(p_a,h_b)$, is calculated in the simplest equispacing model (ESM), without the energy dependent terms or the shell and pairing corrections [18] used in the exciton model and nucleon transfer state densities. Thus,

$$A_{\rm KO}(p_a,h_b) = \frac{1}{2g_a^2}+\frac{1}{2g_b^2}. \quad (5)$$

For inelastic scattering, the particle and hole in the final state are of the same type, and the ESM Pauli correction function is zero. The ESM single particle state densities, g_i, for cluster particle and hole degrees of freedom of type i are related to the values for nucleons according to

$$g_d = (g_{\pi 0}+g_{\nu 0})/4 = (A/52)\,{\rm MeV}^{-1}, \quad (6a)$$

$$g_t = g_h = (g_{\pi 0}+g_{\nu 0})/12 = (A/156)\,{\rm MeV}^{-1}, \quad (6b)$$

$$g_\alpha = (g_{\pi 0}+g_{\nu 0})/16 = (A/208)\,{\rm MeV}^{-1}, \quad (6c)$$

where the proton and neutron single particle state densities are assumed to be

$$g_{\pi 0} = (Z/13)\,{\rm MeV}^{-1}, \quad (7)$$

$$g_{\nu 0} = (N/13)\,{\rm MeV}^{-1}, \quad (8)$$

regardless of what is used in the exciton model calculations. Changing the normalization factor of $g_{\pi 0}$ and $g_{\nu 0}$ would, however, make no practical difference to the results, since it is only ratios of the single particle state densities that enter into the equations for the cross sections. The probabilities $\mathcal{P}_i$ for exciting the different types of particle-hole pairs are given by

$$\mathcal{P}_n = \frac{N_A-\phi Z_A}{A_A-2\phi Z_A+\phi Z_A/2} \cong \frac{N_A}{A_A}, \quad (8a)$$

$$\mathcal{P}_p = \frac{Z_A-\phi Z_A}{A_A-2\phi Z_A+\phi Z_A/2} \cong \frac{Z_A}{A_A}, \quad (8b)$$

$$\mathcal{P}_\alpha = \frac{\phi Z_A/2}{A_A-2\phi Z_A+\phi Z_A/2} \cong \frac{\phi Z_A}{2A_A}, \quad (8c)$$

where ϕ is the fraction of time that four nucleons in correlated orbits will "look like" an α cluster or, alternatively, the fraction of the possible α clusters that will, on average, exist at any given time. It has been assumed that $N\geqslant Z$ so that a maximum of $Z/2$ α clusters is possible. The approximate expressions are obtained assuming that $\phi\ll 1$. Since the size and systematics of ϕ are not well known, the values obtained [19] from radioactive α decay and from (p,α) and (n,α) reactions neglecting pickup were substantially reduced in magnitude and parametrized to give

$$\phi = \begin{cases} 0.08 & \text{for } N_A\leqslant 116,\\ 0.02+0.06(126-N_A)/10 & \text{for } 116<N_A<126,\\ 0.02+0.06(N_A-126)/3 & \text{for } 126\leqslant N_A<129,\\ 0.08 & \text{for } 129\leqslant N_A. \end{cases} \quad (9)$$

The (p,α) and (n,α) values were in remarkable agreement with the radioactive decay results [19], while Hodgson and Běták point out [5] that the reaction values should be significantly lower when the two-component nature of the cluster level density is taken into account. They estimate a factor of six, based on the single particle state densities of the proton, neutron, and α particle, which would put the general size of ϕ (except in the lead region) close to the 0.08 cited above. In practice, the role of α pair excitation turns out to be very small, so the calculated spectra are insensitive to the value of ϕ, so long as $\phi\ll 1$.

The use of a constant normalization factor in Eqs. (2)–(4) inherently assumes—and it is just an assumption—that this

mechanism accounts for the same fraction of the entrance channel cross section for all projectile types at all incident energies. This is open to question. The model is most important for inelastic scattering of complex projectiles, where the intensity relative to that for the exchange of a neutron or a proton with the target needs to be further examined. In particular, it is not clear physically why a weakly bound deuteron or even a triton or ^{3}He should retain its cluster identity during pair excitation to the same extent as the more tightly bound α particle. This issue is discussed more fully in Secs. V C and VIII B.

C. Collective excitations

Finally, excitation of both discrete collective states and giant resonance states in inelastic scattering reactions is now handled using the simple model described in [13]—an adaptation of the model of Kalka *et al.* [20]. These excitations were not included when the nucleon transfer and knockout/inelastic cluster models were developed. They have so far been applied only to nucleon induced reactions but should be applicable for incident complex particles.

III. DATABASE USED

To arrive at reliable phenomenological models, it is vital to have a broad database, in this case one which spans a variety of projectile and ejectile types as well as target masses and incident energies. The current database is listed in Tables I–III and was implemented in stages. The models described above were first revised using only the database from earlier work on complex particle channels. This consisted of energy spectra from proton and α particle induced reactions, taken from the work of Bertrand and Peelle [21,22]. They are indicated by the number 1 in the tables. These spectra were first supplemented by spectra on additional targets for incident protons from the same data sets, with 14.7-MeV $(n, x\alpha)$ spectra [23–25], and, in the case of incident α particles, with spectra that covered a broader range of target masses [26–28]. These are all designated with the number 2 in the tables. Then, after the release of PRECO-2000, data from 90-MeV incident protons [29], and 17- and 50-MeV neutrons [30], were considered, followed by the inclusion of spectra from 140-MeV α particles [31] and then from deuteron [26,32] and ^{3}He [26,33] induced reactions. These are denoted with the number 3. Finally, results were checked and fine-tuned with newly available data for incident neutrons at energies up to 63 MeV on a range of targets [34–38]. These are designated as belonging to stage 4.

At each stage, some features of the formalism from earlier stages were verified and the prescription was made more general. For many of the reaction systems included in this study, (N, xN) spectra are also available and have previously been analyzed [13,39]. These include neutron spectra [40,41] as well as proton spectra measured in conjunction with the complex particle spectra. Many of these (N, xN) results, which are always part of the calculations in PRECO, were checked to make sure that changes in the complex particle channel

TABLE I. Experimental energy spectra for neutron induced reactions used in the current work. The number in the right-hand column indicates the phase of the project in which the data were used.

Projectile	Energy (MeV)	Target	Ejectiles	Reference	Use
n	14.7	^{27}Al	$(n), (p), \alpha$	[23,40]	2
		^{52}Cr	$(n), (p), d, \alpha$	[25,40]	2 (α only)
		^{56}Fe	$(n), (p), d, \alpha$	[25,40]	2 (α only)
		^{93}Nb	$(n), (p), d, \alpha$	[24,40]	2 (α only)
	17	^{28}Si	$(p), d, \alpha$	[30]	3 (α only)
	28.5	^{27}Al	$(p), d$	[34]	4
		^{28}Si	$(p), d$	[35]	4
	29	^{28}Si	$(p), d, \alpha$	[30]	4
	28.5	^{59}Co	$(p), d$	[36]	4
		^{209}Bi	$(p), d$	[37]	4
		^{238}U	$(p), d$	[38]	4
	37.5	^{27}Al	$(p), d, t, \alpha$	[34]	4
		^{28}Si	$(p), d, t, \alpha$	[35]	4
	38	^{28}Si	$(p), d, \alpha$	[30]	4
	37.5	^{59}Co	$(p), d, t, \alpha$	[36]	4
		^{209}Bi	$(p), d, t, \alpha$	[37]	4
		^{238}U	$(p), d, \alpha$	[38]	4
	49	^{27}Al	$(p), d, t, \alpha$	[34]	4
		^{28}Si	$(p), d$	[35]	4
	50	^{28}Si	$(p), d, \alpha$	[30]	3
	49	^{59}Co	$(p), d, t, \alpha$	[36]	4
		^{209}Bi	$(p), d, t, \alpha$	[37]	4
		^{238}U	$(p), d, t, \alpha$	[38]	4
	63	^{27}Al	$(p), d, t, \alpha$	[34]	3
		^{28}Si	$(p), d, t, \alpha$	[35]	3
		^{59}Co	$(p), d, t, \alpha$	[36]	3
		^{209}Bi	$(p), d, t, \alpha$	[37]	3
		^{238}U	$(p), d, t, \alpha$	[38]	3

TABLE II. Experimental energy spectra for proton induced reactions used in the current work. The number in the right-hand column indicates the phase of the project in which the data were used.

Projectile	Energy (MeV)	Target	Ejectiles	Reference	Use
p	29	^{54}Fe	$(p), d, t, {}^3$He, α	[21]	1
		^{120}Sn	$d, t, {}^3$He, α	[21]	2
		^{197}Au	$(p), d, t, \alpha$	[21]	1
	39	^{54}Fe	$(p), d, t, \alpha$	[21]	1
		^{209}Bi	$(p), d, t, \alpha$	[21]	2
	62	^{54}Fe	$(p), d, t, {}^3$He, α	[21]	1
		^{56}Fe	$(p), d, t, {}^3$He, α	[21]	2
		^{89}Y	$(p), d, t, {}^3$He, α	[21]	2
		^{120}Sn	$(p), d, t, {}^3$He, α	[21]	1
		^{197}Au	$(p), d, t, {}^3$He, α	[21]	1
	90	^{27}Al	$(n), (p), d, t, {}^3$He, α	[29,41]	3
		^{58}Ni	$(n), (p), d, t, {}^3$He, α	[29,41]	3
		^{90}Zr	$(n), (p), d, t, {}^3$He, α	[29,41]	3
		^{209}Bi	$(n), (p), d, t, {}^3$He, α	[29,41]	3

TABLE III. Experimental energy spectra for complex particle induced reactions used in the current work. The number in the right-hand column indicates the phase of the project in which the data were used.

Projectile	Energy (MeV)	Target	Ejectiles	Reference	Use
d	24.7	^{63}Cu	p, d, t, α	[26]	3
	70	^{90}Zr	$p, d, t,\ ^3$He, α	[32]	3
		^{208}Pb	$p, d, t,\ ^3$He, α	[32]	3
		^{232}Th	$p, d, t,\ ^3$He, α	[32]	3
	80	^{27}Al	$p, d, t,\ ^3$He, α	[32]	3
		^{58}Ni	$p, d, t,\ ^3$He, α	[32]	3
^{3}He	24.3	^{62}Ni	$p, d, t,\ ^3$He, α	[26]	3
	25.6	^{57}Fe	p	[33]	3
		^{62}Ni	p	[33]	3
		^{116}Sn	p	[33]	3
α	35.5	^{61}Ni	p, d, t, α	[26]	2
	42	^{59}Co	p	[27]	3
		^{103}Rh	p	[27]	3
	54.8	^{56}Fe	α	[28]	3
		^{63}Cu	α	[28]	3
		^{nat}Ag	α	[28]	3
		^{115}In	α	[28]	3
		^{206}Pb	α	[28]	3
	58.8	^{54}Fe	$p, d, t,\ ^3$He, α	[22]	1
	140	^{27}Al	$p, d, t,\ ^3$He, α	[31]	3
		^{58}Ni	$p, d, t,\ ^3$He, α	[31]	3
		^{90}Zr	$p, d, t,\ ^3$He, α	[31]	3
		^{209}Bi	$p, d, t,\ ^3$He, α	[31]	3
		^{232}Th	$p, d, t,\ ^3$He, α	[31]	3

calculations did not significantly disturb the previously obtained agreement.

IV. THE (N, COMPLEX) REACTIONS

It seemed wise to begin the revision of the direct reaction models by considering reactions where the exciton model components could be estimated with the greatest confidence. This, of course, means nucleon induced reactions, and for those reactions, direct pickup is the main mechanism that contributes to complex particle emission. The nucleon induced reactions are relatively insensitive to the α knockout component, which contributes mainly at the very highest emission energies.

A. Direct pickup with incident protons

The particle-hole state densities used in the nucleon transfer calculations are the same as those used in the exciton model. These have been substantially improved since the development of the nucleon transfer model and now include the effects of shell structure, the pairing interaction, and the surface localization of the initial target-projectile interaction. Improved state densities for particle-hole states of a given isospin value are also available for calculations in which isospin is assumed to be conserved. In addition, the normalization factor, K_g, for the proton and neutron single particle state densities

$$g_{\pi 0} = Z/K_g,$$
$$g_{\nu 0} = N/K_g$$

has been changed from $K_g = 13$ MeV to $K_g = 15$ MeV. The last change requires an adjustment of the normalization factor $(2860)^n$ in Eq. (1). This work leads to a value of $(3800)^n$. The really big effect, however, comes from the surface localization of the initial interaction which eliminates the pickup of particles deep in the well and thus drastically reduces the pickup cross section at emission energies well below the ground state transition for incident proton energies at 60 MeV and above.

1. Excitation of additional particle-hole pairs

To compensate for this cutoff, it was necessary to assume that the direct transfer process can be accompanied by the excitation of one or more additional particle-hole pairs—either neutron or proton pairs. An empirical factor, $X_{\rm NT}$, was introduced to give the probability of exciting each additional pair. Thus, the residual state density for nucleon transfer reactions becomes

$$\omega_{\rm NT}(p_\pi, h_\pi, p_\nu, h_\nu, U) = \sum_{i=0}^{3}\sum_{j=0}^{3-i} (X_{\rm NT})^{i+j} \times \omega(p_\pi + i, h_\pi + i, p_\nu + j, h_\nu + j, U), \quad (10)$$

where the excitation of up to three additional particle-hole pairs is allowed. The indices i and j refer, respectively, to the number of proton and neutron pairs excited. The series converges rapidly so that up to incident nucleon energies of 90 MeV, this limit of three additional pairs is more than adequate. Proton projectile data up to 62 MeV indicated only that $X_{\rm NT}$ needs to increase with increasing excitation energy, while including the 90-MeV data shows that an $(E_a)^{1/2}$ dependence is more appropriate than a linear one. It also appears that proton pickup is more effective than neutron pickup at exciting extra p-h pairs, though this conclusion is based largely on the 90-MeV $(p, x\ ^3\text{He})$ spectra. Finally, the empirical normalization of $X_{\rm NT}$ is found to depend on the value assumed for the average effective potential well depth, V_1, in the interaction region of the nucleus. Thus, if the value of V_1 is increased in the calculations, $X_{\rm NT}$ needs to decrease, so that $X_{\rm NT}$ takes on the empirical form

$$X_{\rm NT} = (E_a)^{1/2}\,\frac{7}{V_1\,A_A^2}\left(1.5h_\pi^2 + h_\nu^2\right), \quad (11)$$

where any projectile dependence is still unknown. Again, energies are assumed to be given in MeV.

For consistency, it has been assumed that V_1 is the same effective well depth as is used in the exciton model. For incident protons, $V_1 = 17$ MeV for projectile energies up to around 90 MeV. Differences between the effective well depth at the point of the initial interaction for incident protons and neutrons [13,42] provide a way of testing the assumed relationship between $X_{\rm NT}$ and V_1. As discussed in Sec. IV C, the relationship seems to be a valid one.

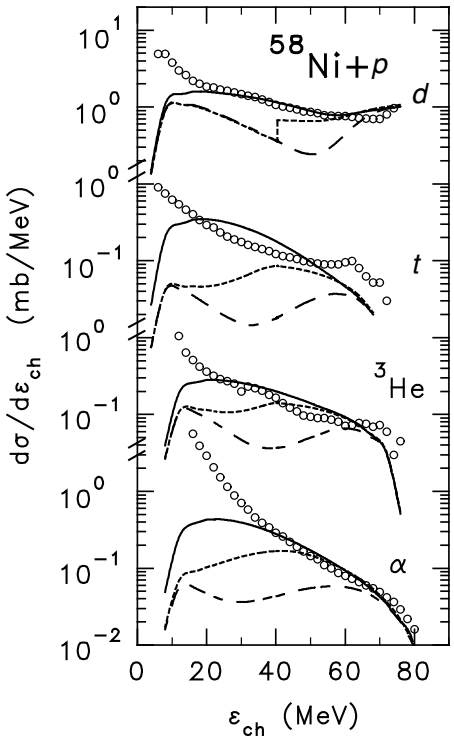

FIG. 1. The importance of allowing extra particle-hole pairs to be excited during direct pickup reactions. The points show the data while the curves show the results of calculations for ^{58}Ni+p at 90 MeV. The solid curves allow extra pair excitation and use the default average effective potential well depth, 17 MeV, at the point of the first interaction. The long-dash curves show the same results without extra pair excitation, while the short-dash curves show how much of the difference can be made up by using the full central well depth of 38 MeV in the nucleon transfer calculations.

It might be argued that the coupling between V_1 and the value of $X_{\rm NT}$ simply indicates that the apparent need for extra pair excitation is an artifact of the way surface localization of the initial interaction is handled in the model, rather than a physical reality. While that is certainly possible, the 90-MeV data seem to require extra pair excitation even when the full well depth of 38 MeV (relative to the Fermi energy) is used in the nucleon transfer calculations. This is shown in Fig. 1. These calculations contain the effects of the smaller changes discussed below. In addition, as is discussed in Sec. V B 2, extra pair excitation is also required in stripping reactions induced by 140-MeV α particles, where the finite well depth does not affect the main nucleon transfer component. Possible explanations for this excitation in both pickup and stripping are discussed in Sec. VI B.

2. Pickup at the Fermi level

Allowing for nucleon transfer at the Fermi surface improves agreement with data, especially on light targets and at the lower incident energies. Nucleons picked up at the Fermi surface do not leave hole degrees of freedom in the residual nucleus, because the Fermi level moves down in going from the target to the residual nucleus. Compared to pickup from random states in the well, the number of excitons in the residual states is lower, as are the energy requirements of the Pauli exclusion principle, which can include the effects of shell and pairing gaps. Such states were not being counted in the residual state densities, even though physically they can be populated. Thus, for multinucleon pickup, the general state densities given above are supplemented by those in which one or more nucleons are picked up at the Fermi level. Since these pickups should occur, including them enhances the realism of the model calculations without introducing additional free parameters. Similar considerations apply in stripping reactions. Bearing in mind that at least one nucleon must be picked up from deeper in the well (or stripped to single particle states well above the Fermi level) in order for there to be at least one degree of freedom to carry the excitation energy in the residual nucleus, the formula for the residual state densities takes on the form

$$\begin{aligned}\omega_{\rm NT}(p_\pi, h_\pi, p_\nu, h_\nu, U) &= \sum_{i=0}^{3}\sum_{j=0}^{3-i}(X_{\rm NT})^{i+j} \\ &\times \omega(p_\pi + i, h_\pi + i, p_\nu + j, h_\nu + j, U) \\ &+ \sum_{i=0}^{p_\pi}\sum_{j=0}^{h_\pi}\sum_{k=0}^{p_\nu}\sum_{l=0}^{h_\nu}\omega(p_\pi - i, h_\pi - j, p_\nu - k, h_\nu - l, U) \\ &\times \Theta\left(i + j + k + l - \frac{1}{2}\right). \end{aligned} \quad (12)$$

Here, Θ is the Heaviside function, which is unity for a positive argument and zero for a negative one. This change has the effect of filling in the calculated energy spectra at the highest emission energies, near the ground-state transition, and uniformly improves agreement with experiment.

3. Transfer of nucleon pairs

Another change which represents physical reality and adds no free parameters is to allow for two neutrons or two protons to be transferred with their spins paired. This reduces the pairing energy correction in the residual nucleus when the transfer occurs on a target with even Z (for two-proton transfer) or even N (for two-neutron transfer). This is found to improve agreement with experiment for light targets at low bombarding energies and is most clearly seen in 14-MeV (n, α) reactions, which are considered in Sec. IV C.

4. Extra surface localization of pure neutron pickup

With additional energy spectra available for a wide range of target masses, the problem of reproducing the relative yields, particularly in the triton and ^{3}He channels, is particularly evident. It occurs at 90 MeV as well as at 62 MeV, even though the data were taken at different times by different laboratories. To correct this and improve agreement generally, it is assumed that a large neutron excess in the target allows pickup (and even stripping) involving only neutron transfer to occur, on average, further out toward the nuclear surface. This could be due to a neutron-rich region at the nuclear surface. Thus, the average

effective well depth used in the nucleon transfer calculations is reduced by the factor $(2Z/A)$ for purposes of calculating the finite well depth corrections to the state densities (but not in evaluating $X_{\rm NT}$).

B. Isospin conservation

Most of the complex particle emission spectra studied are insensitive to the assumptions made about the extent of isospin mixing in the preequilibrium phase of the reaction. Thus, these assumptions do not affect the empirical form of the models. On the other hand, it was found to be important to assume full mixing of isospin in reproducing the relative intensities in the various exit channels in several reactions on light targets. This results largely from the isospin coupling Clebsch-Gordan coefficients in the entrance and exit channels. A similar sensitivity was found later for α particle induced reactions. This information supplements that from preequilibrium studies of (N, N) reactions and is discussed in a separate paper on isospin conservation [43]. The overall criterion for isospin conservation in the preequilibrium phase of the reaction that is assumed in this work is taken from those studies and is $E < 4E_{\rm sym}$, where $E_{\rm sym}$ is the isospin symmetry energy in the composite nucleus. When isospin is conserved during the preequilibrium phase, it is also assumed to be 40% conserved at equilibrium, except for systems where the excitation energy is close to $4E_{\rm sym}$.

The way that isospin conservation is treated in the exciton model is discussed in [10]. It is included in an analogous way in the nucleon transfer model, using residual state densities with good isospin, including the entrance and exit channel Clebsch-Gordan coefficients, and considering all allowed isospin couplings.

C. Pickup with incident neutrons

The treatment of nucleon transfer reactions with incident neutrons should follow fairly directly from the results for incident protons, but several open questions remain to be answered. They are: the overall normalization (is it the same?); whether $X_{\rm NT}$ is truly proportional to $1/V_1$; and verification of the exponent in the term $(2Z_A/A_A)^{6n_\pi}$ when $n_\pi = 2$. For proton induced reactions, only $n_\pi = 0, 1$ occur. In addition, it may be possible to extract extra or confirming information on the values of V_1 from some of the complex particle spectra.

1. Normalization

First, is the incident proton normalization of $3800^n/80$ also appropriate for incident neutrons? Because of uncertainties concerning how the amount of surface localization of the initial interaction might affect the excitation of additional particle-hole pairs during pickup, the normalization was set using deuteron and α spectra for bombarding energies of 29 and 38 MeV, where extra pair excitation is not important. Similarly, only the ^{28}Si target, with $N = Z$, was considered so that uncertainties in the exponent of the $2Z/A$ factor do not apply.

These studies indicate that the overall normalization of 1/80 is probably valid but that the numerator in the term $(3800/A_B)^n$ needs to be increased. The α spectra are more sensitive to this term than the deuteron spectra because they involve the transfer of three nucleons ($n = 3$) rather than just one. A factor of about $(5500/A_B)^n$ is indicated.

2. Form of $X_{\rm NT}$ for extra pair excitation

It is now time to consider new evidence on the relationship between the factor $X_{\rm NT}$ and the average potential well depth in the interaction region. A recent investigation [42] found evidence for a difference in $V_{\rm eff}$ values obtained from (n, xn) and (n, xp) spectra. The values obtained are

$$V_{{\rm eff},nn} = 7\ {\rm MeV}, \tag{13a}$$

$$V_{{\rm eff},np} = \min\left(7\ {\rm MeV} + 5.2\,E_{\rm inc}\left[\frac{N-Z}{A}\right]^2, V_0\right). \tag{13b}$$

Since for incident protons $V_{\rm eff} = 17$ MeV at incident energies up to around 90 MeV, and since it is assumed that in direct pickup reactions $V_1 = V_{\rm eff}$, the different neutron values of $V_{\rm eff}$ provide an opportunity to see if V_1 was a meaningful parameter to include in Eq. (11). This is done for the light targets ^{28}Si and ^{27}Al, for which $V_{{\rm eff},np} \cong V_{{\rm eff},nn} = 7$ MeV and the $2Z/A$ factor in the formula for the nucleon transfer cross section is 1 or close to 1. The exponent of that latter term is considered below, and results from the heavier targets are then used to study the possibility of verifying Eq. (13b).

The silicon and aluminum data at incident energies of 49–63 MeV were compared with calculated results obtained by evaluating $X_{\rm NT}$ using either $V_1 = V_{\rm eff} = 7$ MeV, as in the exciton model calculations, or 17 MeV, as for incident protons. Where the experimental results indicate a clear choice, it always favors the use of $V_1 = V_{\rm eff} = 7$ MeV, so the tentative choice of using V_1 in Eq. (11) based on the behavior of the proton induced reactions seems to be confirmed. The sensitivity to this choice is shown in Fig. 2. The possibility of verifying Eq. (13b) from results on complex particle emission from heavier targets is evaluated in Sec. IV D.

3. Exponent of the 2Z/A factor

Work on proton induced reactions suggested that the exponent on the factor $2Z/A$ in Eq. (1) is $6n_\pi$, but only values of $n_\pi = 0, 1$ were available. With incident neutrons, the (n, α) reaction gives the opportunity to probe reactions with $n_\pi = 2$. To investigate this exponent, the complex particle spectra resulting from 63-MeV neutrons incident on targets of cobalt, bismuth, and lead were investigated. It soon became apparent that the exponent for $n_\pi = 1$, as well as that for $n_\pi = 2$, needed to be reduced from the starting value of $6n_\pi$. Comparisons of the initial calculations with the data were used to estimate the desired exponent on this term, and the results are shown in Fig. 3. The indicated exponents from the deuteron and triton spectra ($n_\pi = 1$) are similar to one another and lower

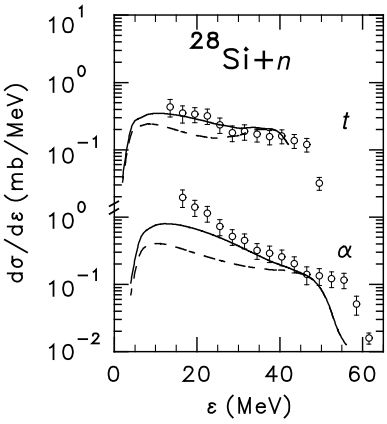

FIG. 2. Sensitivity of the data from neutron induced reactions to the form of $X_{\rm NT}$, the factor reducing the state densities for extra pair excitation in nucleon transfer. The results are for ^{28}Si+n at 62.7 MeV. The points show the data as a function of laboratory energy, while the curves show the calculated results versus channel energy. The solid curves assume that $X_{\rm NT}$ is proportional to $1/V_1$, while the dashed curves replace this dependence with the proton value of 1/(17 MeV).

than the exponents from the α spectra ($n_\pi = 2$). Together, they indicate that the exponent in Eq. (1) needs to be different for proton and neutron induced reactions and, therefore, must have a dependence on Z_a, the atomic number of the projectile.

The results in Fig. 3 plus the proton results can be approximated by various formulae. However, restricting the exponents to integer values and requiring them to depend on the number of picked up protons but not neutrons, as indicated by the proton induced reactions, severely limits the choices. Assuming, for simplicity, a linear dependence on n_π leads to an exponent of $2(Z_a + 2)n_\pi$, which gives the dashed lines in Fig. 3.

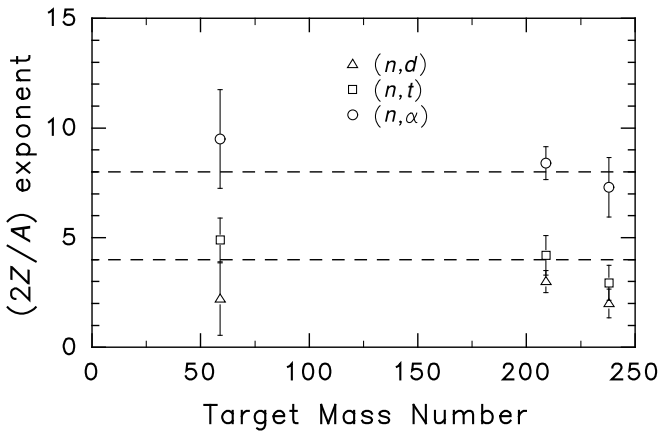

FIG. 3. Empirical values for the exponent of the factor $2Z/A$ in the cross section for neutron induced direct pickup reactions at 62.7 MeV. These are displayed as a function of target mass number for clarity. The adopted values are shown as dashed lines.

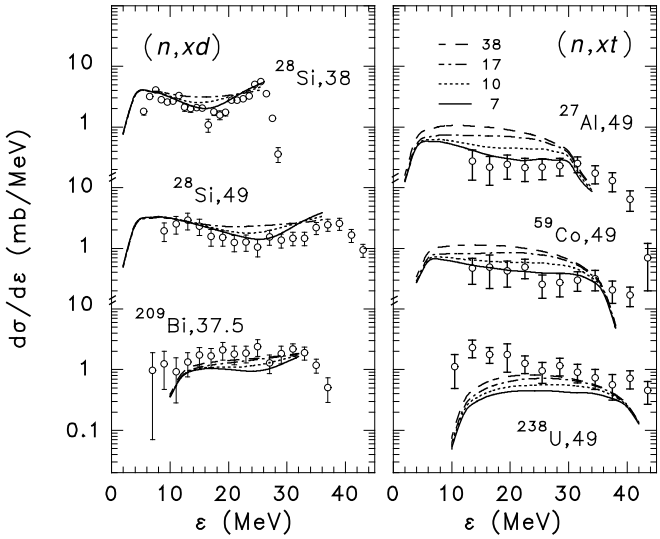

FIG. 4. Sensitivity of the complex particle energy spectra to the assumed value of $V_{{\rm eff},nn} = V_{{\rm eff},np} = V_1$ in the exciton model and nucleon transfer reaction calculations. The points show the data as a function of laboratory energy (except for ^{28}Si at 38 MeV, where it is channel energy), while the curves show the calculated results versus channel energy for the indicated well depths at the point of the first target-projectile interaction. The curves are labeled with the target nucleus and incident energy.

D. Surface localization for incident neutrons

Finally, it is worth seeing if Eq. (13b) can be confirmed. Since pickup reactions with incident neutrons always involve the transfer of at least one proton, Eq. (13b) is used for nucleon transfer reactions while Eqs. (13a) and (13b) are used for the initial *nn* and *np* interactions, respectively, in the exciton model.

The data at higher energies are those most sensitive to variations in $V_1 = V_{{\rm eff},np}$, because the limitations imposed by the finite well depth grow as the incident energy increases. These data have been used to look for evidence supporting the target dependence of Eq. (13b). In this investigation, many of the (n, xd) spectra show sensitivity in the spectral shape, while the (n, xt) spectra and some of the $(n, x\alpha)$ spectra show sensitivity in their intensity. Figure 4 shows sample spectra when the values of $V_{{\rm eff},nn} = V_{{\rm eff},np} = V_1$ are varied in the reaction calculations. Previously, the aluminum and silicon spectra were used only in verifying the V_1 dependence of $X_{\rm NT}$ and thus can provide useful insights. The 63-MeV spectra for the heavier targets were, however, used to set the exponent for $2Z/A$ in the nucleon transfer model, so that spectral shape information is most useful here. Arguing from intensities for these targets is only useful when the $2Z/A$ exponent and variations in V_1 have different effects on the relative intensities of the different exit channels. While the data do not allow accurate values of $V_{\rm eff}$ to be estimated, they do confirm the general trend noted in [42] for $V_{\rm eff}$ to increase with increasing target mass or neutron excess, and they show that the values extracted from the proton emission spectra work well for the complex particle spectra as well.

It can still be argued that for heavy targets there is a strong coupling between the exponent of $2Z/A$ and the value of V_1 whenever V_1 has a significant effect on the intensity of the nucleon transfer component. In principle this is true. However, the $2Z/A$ factor enters equally in the (n, d) and (n, t) nucleon transfer components. For the bismuth and uranium targets, these are the dominant components in the high-energy half of each spectrum, and so the $2Z/A$ factor has similar effects on the two channels. Yet, the (n, xd) spectra for these targets at 49 and, especially, 63 MeV are remarkably insensitive to V_1, while the (n, xt) spectra are far more sensitive. This enables the two effects to be largely untangled. In addition, the main effect of V_1 for the (n, d) pickup is one of shape and not intensity. Thus, the consistency of the picture that is emerging suggests both that the change in the $(2Z/A)$ exponent is needed and that the $V_1 = V_{\text{eff},np}$ values given by Eq. (13b) give a more consistent description of the data than assuming an invariable value of 7 MeV.

At lower incident energies, the error bars on the Louvain data are larger, and the sensitivity to V_{eff} decreases. Thus, it is not possible to confirm the incident energy dependence of Eq. (13b).

V. REACTIONS WITH COMPLEX PROJECTILES

With complex projectiles, a greater variety of preequilibrium mechanisms can contribute to emission of a particular type of particle than is the case with nucleon projectiles. Separating the contributions from these different mechanisms is often an ambiguous process. Further, the exciton model parameters are not known as well for complex projectiles. The approach taken has been to start with the models used for incident nucleons, assume that the same parameters are applicable for complex particles, and look for places where the nature of the projectile makes changes necessary. Those changes need to be systematic, so that they work for d, ^{3}He, and α particle projectiles and for all light particle exit channels. This puts severe constraints on what will work.

In this way, it is possible to arrive at a useful, working phenomenology, but these reactions are not yet understood or described as satisfactorily as the nucleon induced reactions. In particular, there is evidence from both angular distributions [44] and spectral shapes that projectile breakup contributions can be important. Thus, complex particle induced reactions will need more careful study with the inclusion of projectile breakup before they can be described with confidence. With these limitations in mind, here is what has been achieved.

A. Exciton model parameters for complex projectiles

1. The mean square matrix elements

There is really only one important parameter in the exciton model that is not at least approximately determined from other sources: the effective mean square matrix element for the residual two-body interactions that bring about energy equilibration. The incident energy and target mass dependences have been determined empirically from nucleon induced reactions, as have the overall normalization and the relative normalizations for nn, np, and pp interactions. One would hope that the size of the matrix elements would be independent of the projectile, but since these are effective parameters, that need not be the case. A projectile dependence could be needed to compensate for approximations or inadequacies elsewhere in the calculations.

Indeed, the first comparisons of PRECO results with continuum spectra for α particle induced reactions at 59 MeV showed that the calculated preequilibrium intensity in the (α, xp) channel was significantly too high and that most of the excess occurred in the exciton model calculations. Setting the nucleon transfer and (α, p) knockout contributions to zero would still leave the calculations above the measured spectra for a range of emission energies. This implies that the residual two-body matrix elements used in the calculation were too small, allowing too much preequilibrium emission to occur. Larger matrix elements lead to more pair creation interactions, which take the system toward equilibrium and compete with particle emission. The form for the mean square matrix elements was [11]

$$M_{ij}^2 = K_{ij} A^{-3} (20.9 + E/3)^{-3}, \tag{14}$$

where the factor of 3 occurring in the denominator replaces an earlier factor of n, the exciton number, based on comparisons with data on (N, xN) reactions at 25 and 90 MeV. The subscripts i and j refer to the type of nucleons (neutrons or protons) involved in the interaction, and the K_{ij} are empirical normalization constants [12].

Replacing the excitation energy, E, with the energy per projectile nucleon, E/A_a, helps and is better than returning to the old E/n form, but it is still inadequate for the (α, xd) and (α, xt) spectra up to 60-MeV incident energy. Various forms have been tried, but the one that seems to give reasonable overall agreement for complex projectiles (d, ^{3}He, and α) over a wide range of incident energies is

$$M_{ij}^2 = K_{ij} A_a A^{-3} (20.9 + E/3A_a)^{-3}. \tag{15}$$

This form has therefore been provisionally adopted. Figure 5 shows some sample spectra compared with the exciton model components calculated with (14), (15), and (15) without the extra factor of A_a.

Breakup contributions still need to be included in PRECO, along with the emission produced whenever the undetected breakup fragment interacts with the target to begin an exciton model calculation. This should be most important for d and, to a lesser extent, ^{3}He projectiles, and might require further modifications in M^2. Figure 5 shows an estimate of the (d, p) breakup contribution based on preliminary systematics derived from breakup components reported in the literature. It has not been added to the calculated results from PRECO.

2. Initial configuration for particle emission

It is currently assumed that a complex projectile breaks up during the first particle-hole pair excitation. The exciton model calculations are started with a configuration $(p_\pi, h_\pi, p_\nu, h_\nu) = (Z_a, 0, N_a, 0)$, which looks as if the

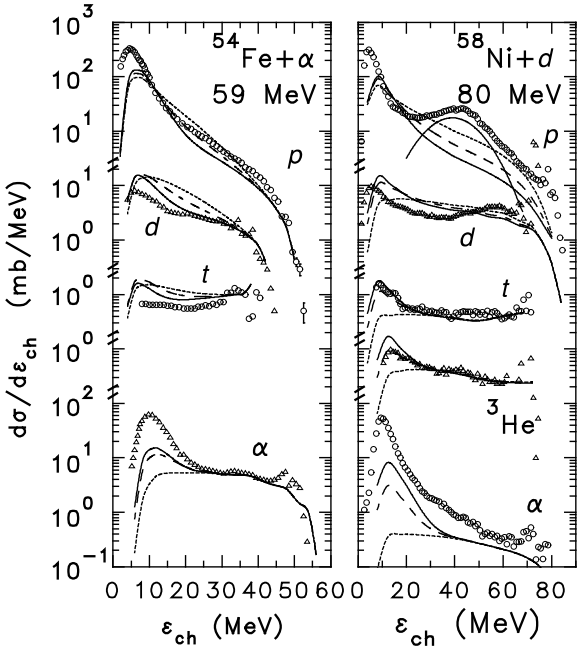

FIG. 5. Sensitivity of the calculations to the assumed form of the mean square matrix element in the exciton model. The short-dash, long-dash, and solid curves correspond, respectively, to Eqs. (14), (15) without the extra factor of A_a, and (15). The points show the data.

projectile were dissociated, but this is done only in order to get the right balance between pp, pn, and nn interactions in the first pair creation. Particle emission is first allowed from the states produced in that interaction, i.e., the $(Z_a + 1, 1, N_a, 0)$ and $(Z_a, 0, N_a + 1, 1)$ configurations.

The choice to allow particle emission to occur only after pair creation was made [16] using a much earlier version of the models and a very limited database. Now, with the larger matrix elements for complex projectiles reducing the intensity of the exciton model components, there is reason to reconsider this choice. When this is done, it is clear that allowing particle emission to begin from configurations with $(Z_a, 0, N_a, 0)$ often yields too much high energy nucleon emission for deuteron and ^{3}He projectiles. However, at least for incident deuterons and ^{3}He, projectile breakup should significantly reduce the amount of the total reaction cross section that would be available to the exciton model calculations, further lowering the exciton model components and leaving room for the simpler initial configuration with its higher emission rates.

Additional evidence is seen in Fig. 5, which shows that there is too little cross section above the breakup peak in the (d, xp) spectrum—the region that would be most filled in by allowing particle emission to occur prior to the first pair excitation. This is a general trend for deuteron and ^{3}He induced proton emission. Finally, there might seem to be some inconsistency in assuming a large projectile breakup cross section (without pair excitation) and also assuming that in the exciton model a complex projectile dissociates only *after* pair creation. Both processes could still be going on, for instance, at different impact parameters, but allowing dissociation before pair creation would seem to be a reasonable assumption within the exciton model, at least for loosely bound projectiles.

Preliminary calculations seem to show that once the cross section available to the exciton model calculations is reduced by an appropriate amount for projectile breakup, it is not only reasonable to assume that particle emission can occur from an initial configuration of $(Z_a, 0, N_a, 0)$, but agreement with experiment will likely be improved by doing so. Since a full study of the breakup component has not yet been carried out, the calculations in this paper will continue to assume that particle emission occurs only after the first pair creation interaction.

B. Revising the nucleon transfer model

1. Pickup reactions

The most encouraging aspect of the complex particle induced reactions is that the pickup channels—(d, t), $(d, ^3\mathrm{He})$, (d, α), and $(^3\mathrm{He}, \alpha)$—all seem to be reasonably well described by the model developed for nucleon induced pickup using the normalization for proton induced reactions. For incident energies around 25 MeV, no modifications are needed, while for deuterons at 70–80 MeV, extra pair excitation becomes important and the values for X_{NT} are adequate but not optimal, particularly for the triton to ^{3}He yield ratios. This aspect of complex particle induced pickup is discussed below, along with extra pair excitation in direct stripping.

2. Stripping reactions

For stripping reactions, the cleanest and most complete data set is for α particle induced reactions. The inclusive spectra at 140 MeV [31] cover a broad range of targets, while adding the data from the Fe-Ni region at 35.5 [26] and 58.8 [22] MeV provides for a range of incident energies. In each case, all or all but one of the light charged particle exit channels were studied. In addition, any breakup components should be significantly smaller than in the (d, p) reactions at 70 and 80 MeV.

A number of modifications to the nucleon transfer formalism are needed for the α induced reactions. Previously, the same equations were used for both stripping and pickup because they appear to be time-reversed processes and because the data were insufficient to indicate the need for a difference. Now, with the inclusion of the 140-MeV projectile data, it appears that the cross section normalization factor $(80E_a)^{-1}$ used for pickup needs to become $(580\sqrt{E_a})^{-1}$ for stripping. The two are equivalent for an incident energy of around 52 MeV, while at higher energies the stripping normalization is larger than that for pickup.

Another change for the main stripping component is a reduction in the enhancement factor for (α, N) reactions as the incident energy increases relative to the 20-MeV internal binding energy of the α particle. This is reasonable since the enhancement factor was thought to reflect the greater stability of the nucleon and α particle relative to the more weakly bound deuteron, triton, and ^{3}He. With this explanation in mind, the

new form of $K_{\alpha,p}$ was set to be

$$K_{\alpha,p}=\begin{cases}12 & \text{for } (N,\alpha),\\ 12 & \text{for } (\alpha,N) \text{ and } \varepsilon_a < 20,\\ 12-11(\varepsilon_a-20\ \text{MeV})/\varepsilon_a & \text{for } (\alpha,N) \text{ and } \varepsilon_a > 20,\\ 1 & \text{otherwise,}\end{cases} \tag{16}$$

and this simple prescription seems to work well at 35, 42, 59, and 140 MeV. The quantity 20 MeV in this equation was chosen because it is the average binding energy of a nucleon in the α particle.

The last normalization question is the exponent of the factor $(2Z_A/A_A)$ in Eq. (1), which could not previously be investigated for stripping because the data did not contain a broad range of target masses. This factor was thought to represent a hindrance to proton pickup at the nuclear surface from nuclei with a large neutron excess. If this is the case, then there should be, if anything, a hindrance to neutron stripping because more of the neutron states in the residual nucleus are occupied. At present, the 140-MeV α data suggest that in order to reproduce the measured relative yields of tritons and ^{3}He, an exponent of 2 is appropriate for the $(\alpha, {}^3\text{He})$ reaction. Assuming that this represents an exponent of $2p_\nu$, the same exponent generally works for the (α, d) reactions at 140 MeV and for the high emission energies in the (α, p) spectra, though the ^{209}Bi spectra are somewhat overcorrected.

3. Extra pair excitation

For stripping reactions, it is mainly the data for 140-MeV incident α particles that are sensitive to $X_{\rm NT}$. Here, a significant reduction from the nucleon projectile values is needed, though it is also evident that setting $X_{\rm NT}=0$ is not an option since it leaves vast amounts of cross section in the middle of the spectra unaccounted for.

A reasonable change is to adjust the value of V_1, the effective well depth at the point of interaction. Since a base value of $V_1=7$ MeV is indicated for incident neutrons (changing to higher values for charged particle emission from heavy targets as the incident energy increases), and a value of 17 MeV is indicated for incident protons and deuterons, it would be reasonable to expect a larger value for incident ^{3}He and α particles, since the Coulomb forces are larger. Unfortunately, the residual states from the main stripping component are insensitive to the finite well depth, so this number cannot be determined directly from the spectral shapes. If $(E_a)^{1/2}$ is changed to $(E_a/A_a)^{1/2}$ in $X_{\rm NT}$, then using $V_1=25$ MeV provides improved agreement with experiment for the 140-MeV α particle data. This value of V_1 seems reasonable when compared to the values for other projectiles. On the other hand, if the factor $(E_a)^{1/2}$ is left alone, then it is necessary to use a well depth of about 50 MeV in order to get the correct amount of additional pair excitation—assuming again that V_1 really is the physical quantity involved in $X_{\rm NT}$. But 50 MeV is significantly higher than the currently assumed central well depth of 38 MeV relative to the Fermi level. Thus, it is provisionally assumed that $X_{\rm NT}$ depends on $(E_a/A_a)^{1/2}$ for all light projectiles and that $V_1=25$ MeV for incident α particles and ^{3}He.

In addition, it is necessary to determine the relative efficacy of proton and neutron stripping for exciting extra particle-hole pairs. Analogy with proton induced pickup would suggest $X_{\rm NT}\propto(1.5p_\pi^2+p_\nu^2+1.5h_\pi^2+h_\nu^2)$. The relative yields of tritons and ^{3}He suggest that the factor of 1.5 be eliminated for proton stripping. The (α, d) spectra are less sensitive but tend to support this conclusion, while the (α, p) spectra are less sensitive still. Thus, the factor of 1.5 in front of the term in p_π^2 has been dropped, so that $X_{\rm NT}\propto(p_\pi^2+p_\nu^2+1.5h_\pi^2+h_\nu^2)$, and the form adopted for $X_{\rm NT}$ becomes

$$X_{\rm NT}=\left(\frac{E_a}{A_a}\right)^{1/2}\frac{7}{V_1\,A_A^2}\left(p_\pi^2+1.5h_\pi^2+p_\nu^2+h_\nu^2\right). \tag{17}$$

Now we can return to the question of extra pair excitation in deuteron induced pickup reactions at 70–80 MeV. Using Eq. (17) for $X_{\rm NT}$ and the proton value $V_1=17$ MeV (which is assumed for all deuteron induced reactions) results in lowering the amount of extra pair excitation relative to using Eq. (11), and the results are generally reasonable. The biggest difficulty is that for the heavier targets, triton emission and, to a lesser extent, α particle emission seem to be underestimated in the middle of the spectra. The triton spectra could probably be remedied by removing the extra surface localization for pure neutron pickup introduced in the study of proton induced reactions. There, the effective well depth was reduced by a factor of $(2Z_A/A_A)$ for pure neutron pickup. This reduction has been retained for consistency with the treatment of proton induced reactions. This question, however, may need to be revisited when more data become available and after projectile breakup and its influence on the exciton model calculations have been taken into account.

4. Exchange reactions

Using different incident energy dependencies for pickup and stripping reactions raises the question of what to do for exchange reactions, where one nucleon is stripped and another is picked up. These processes were previously calculated only for d and ^{3}He projectiles and would contribute to the inelastic channels through exchange of a neutron or a proton and to the $(^3\text{He}, t)$ reaction. In the (d, d') and $(^3\text{He}, ^3\text{He}')$ reactions, the nucleon exchange component is only 10–15% of the calculated direct cluster inelastic scattering, so the exchange component cannot be studied effectively. There is only one data set that includes $(^3\text{He}, t)$: the ^{62}Ni+^{3}He system at 24.3 MeV [26]. At this energy, the calculations are insensitive to the finite well depth corrections and to extra pair excitation. Of the two normalizations, the one for stripping (the smaller of the two) seems to give better agreement with the data, though the calculated intensity is still about a factor of 2 too high, and the results are insensitive to assumptions about isospin conservation. This is a minor channel, accounting for only 1.5% of the total reaction cross section, and it would be premature to make any changes to the phenomenology based on one spectrum. Further evidence on the normalization is considered below.

Two other questions remain: Should nucleon exchange be allowed to contribute to (α, α') reactions, and should extra pair excitation be considered in exchange reactions?

Since extra pair excitation is allowed—and, indeed, needed—for both pickup and stripping reactions, reasons of consistency would seem to demand that it be included for exchange processes. Allowing it to contribute to the (d, d') reactions at 70 and 80 MeV shows that the agreement with experiment becomes a bit worse at intermediate emission energies, especially for the ^{58}Ni target. For incident energies around 25 MeV, the effect is minimal. This change could be somewhat compensated for by reducing the normalization of the components involving cluster degrees of freedom, which are discussed in the next section.

Again, since stripping reactions are allowed and necessary for α-particle projectiles, consistency would demand that inelastic exchange also be allowed. Adding inelastic exchange without extra pair excitation for the (α, α') reactions causes no major problems. The calculated cross section is increased somewhat, but an adjustment in the overall normalization of the models in Sec. V C would easily compensate. That normalization was determined largely from (α, α') reactions and could readily be reduced. The problem arises when extra pair excitation is included. Then, for the 140-MeV data, the sum of the calculated direct reaction components becomes comparable to the total reaction cross section for ^{27}Al and ^{90}Zr, and it exceeds the total reaction cross section for ^{58}Ni. In addition, the calculated $(\alpha, x\alpha)$ spectrum is too intense at intermediate emission energies. Thus, simply reducing the normalization for the flatter cluster-inelastic spectrum is unlikely to be adequate.

Another possibility is suggested by the ^{62}Ni(^{3}He, t) reaction at 24.3 MeV, where a reduction in the charge exchange normalization of about a factor of 2 would be needed to give agreement with experiment. Applying that same reduction to all of the exchange channels would eliminate the problem of the excessive direct reaction cross sections for 140-MeV α particles (though just barely for ^{58}Ni) and would generally help agreement with experiment. A small renormalization of the model for cluster-inelastic scattering would still be possible. This change has been implemented, making the nucleon transfer normalizations

$$\mathcal{N}_a = \begin{cases} (80\varepsilon_a)^{-1} & \text{for pickup,} \\ (580\sqrt{\varepsilon_a})^{-1} & \text{for stripping,} \\ (1160\sqrt{\varepsilon_a})^{-1} & \text{for exchange.} \end{cases} \quad (18)$$

Obviously, it would be good to have a confirmation of the normalization difference between stripping and exchange. This will, however, require additional data on (^{3}He, t) or (t,^{3}He) reactions at a variety of energies on a wide range of targets. For these reactions, the only other preequilibrium component that needs to be considered is due to the exciton model.

With inelastic exhange considered for all of the light complex projectiles, it was also included for incident nucleons. However, the contribution is so small that it makes no practical difference to the calculated spectra.

C. Revising the models with cluster degrees of freedom

The model for inelastic scattering and knockout processes involving cluster degrees of freedom is assumed to account for a major part of inelastic scattering spectra for projectiles with $A = 2$–4. The normalization was previously adjusted to $C_a = 1/12$, based on the (α, α') spectra at 35.5, 54.8, and 59 MeV. With all the additional changes made in the nucleon transfer components, with the addition of the 140-MeV (α, α') spectra, and especially with the inclusion of the nucleon exchange inelastic contribution for α particles, an additional adjustment to the normalization is possible. No single number is optimal for all cases, but overall, a normalization of $C_a = 1/14$ seems appropriate.

This raises a question: Is it reasonable to assume that a loosely bound deuteron or ^{3}He could retain its cluster identity during pair excitation, at least to the same extent as an α particle? That is the current assumption. Thus, the calculations in PRECO currently have the projectile dissociating before pair creation in the breakup mechanism, during pair creation in the exciton model, and not at all in cluster scattering. This issue is discussed further in Sec. VIII B, where possible future approaches to this question are considered.

D. The collective excitation model

In order to verify the simple collective excitation model used here, spectroscopic data for a few individual states have been studied, but this requires the use of angular distributions. For incident nucleons, the general trend of the angular distributions for collective excitations, averaged over the diffraction maxima and minima, has been assumed [13] to roughly follow the global systematics [45] used in other preequilibrium calculations. In these systematics, the angular dependence of the double differential cross section is expressed as an exponential in $a_{\rm ex}\cos\theta$, where $a_{\rm ex}$ is the so-called slope parameter for the exciton model and related parts of the calculation. This behavior was verified both for collective states and for the backward-hemisphere component of elastic scattering, using data for 14-MeV neutrons [46] and 39–62-MeV protons [21]. The sample comparisons in Fig. 6 also show that the magnitude of the collective cross sections is reasonably well accounted for using the collective state parameters given in [13].

Similar comparisons have been carried out for complex projectiles. Results for incident deuterons at 80-MeV [47] and α particles at 30 [48] and 43 [49] MeV have been studied for collective states, along with elastic angular distributions from deuterons at 15, 21.6, and 80 MeV [47,50], tritons at 20 MeV [51], ^{3}He at 21 MeV [52], and α particles at 24.7 and 40 MeV [53,54]. The results uniformly indicate that the collective (and back angle elastic) angular distributions are far more forward peaked than the general systematics, would predict. Though there are a few reactions where the data show a significantly different behavior, in general, an adequate description for each projectile type can be obtained by multiplying the usual slope

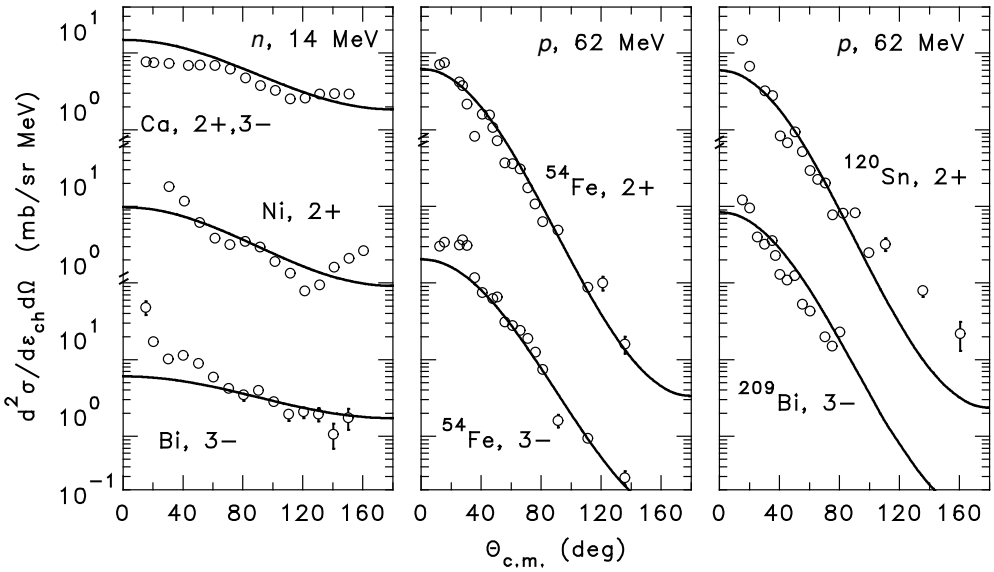

FIG. 6. Comparison between calculation and experiment for collective state angular distributions in nucleon inelastic scattering. The points show the data of [46] and [21], while the curves show the results obtained using the collective model in PRECO and the global angular distribution systematics for continuum reactions.

parameter by a projectile-dependent factor. These factors are roughly

Projectile	Slope parameter multiplier
d	1.5
t	1.9
^{3}He	1.5
α	4.3

While the number for α particles looks substantially higher than the others, that is partly illusory. α particles are the only light projectile where the empirical relationship for the main slope parameter has two terms rather than three. If the third term were used for α particles and had the same size as for nucleons and deuterons (the size assumed for tritons and ^{3}He), then the α collective multiplier would be 1.9. The same systematics are assumed to apply to giant resonance states and should help explain the forward angle component in α inelastic scattering observed in [44]. While these numbers are tentative and approximate, and while the angular range of the data is quite limited, the new systematics permit a comparison in magnitude between calculation and experiment. Sample fits to collective excitations are shown in Fig. 7.

The magnitude of the calculated cross section is dependent on the assumed value for β_λ. The values tabulated in [13] generally produce calculated cross sections that are lower than the smoothed trend of the experimental values, though the factor is variable (1–2.5) with an average of about 1.5. This factor has not been added to the model.

VI. STATUS AND DISCUSSION OF MODEL CHANGES

A. Status of models

The only change made in the exciton model calculations is adding a projectile mass number dependence to the mean square matrix element for the residual two-body interactions responsible for energy equilibration. The new expression for these quantities is given in Eq. (15). Currently, particle emission is assumed to occur only after excitation of the first particle-hole pair, but once a model for the breakup of complex projectiles is included in the calculations and is allowed to reduce the cross section available to the exciton model, it is likely that allowing the projectile to dissociate into its constituent nucleons prior to pair excitation will yield better agreement with experiment. In this case, particle emission

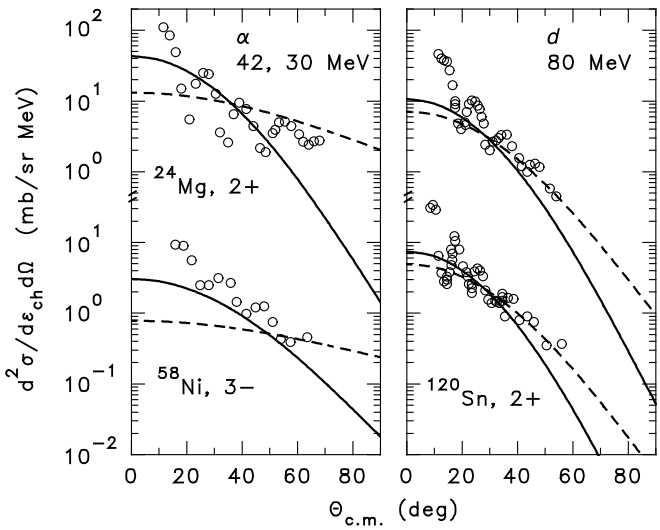

FIG. 7. Comparison between calculation and experiment for collective state angular distributions in complex particle inelastic scattering. The points show the data of [47–49]; the dashed curves show the calculated results with the global angular distribution systematics; and the solid curves show the results with the adjusted slope parameter.

would occur from the $(p, h) = (A_a, 0)$ initial states. The latter assumption is more consistent with a prominent projectile breakup contribution to reactions induced by deuterons and ^{3}He.

The summary formula for nucleon transfer as it is emerging from this work shows more projectile dependence than was evident with the earlier, more restricted database. It also has much greater predictive ability for reactions at higher energies or with complex projectiles. It allows for the excitation of extra particle-hole pairs during nucleon transfer, for the transfer of two protons or two neutrons with their spins paired, and for pickup or stripping from the Fermi level. The formula is

$$\left[\frac{d\sigma_{a,b}(\varepsilon)}{d\varepsilon}\right]_{\mathrm{NT}} = \frac{2s_b+1}{2s_a+1}\,\frac{A_b}{A_a}\,\frac{\varepsilon\,\sigma_b(\varepsilon)}{A_a}\,K_{\alpha,p}\left(\frac{A_a}{E_a+V_a}\right)^{2n}\left(\frac{C_a}{A_B}\right)^{n} \times \mathcal{N}_a \sum_{p_\pi}\left(\frac{2Z_A}{A_A}\right)^{2(Z_a+2)h_\pi+2p_\nu} \omega_{\mathrm{NT}}(p_\pi, h_\pi, p_\nu, h_\nu, U), \tag{19}$$

where

$$C_a = \begin{cases} 5500 & \text{for incident } n, \\ 3800 & \text{for charged projectiles,} \end{cases}$$

$$\mathcal{N}_a = \begin{cases} (80\varepsilon_a)^{-1} & \text{for pickup,} \\ (580\sqrt{\varepsilon_a})^{-1} & \text{for stripping,} \\ (1160\sqrt{\varepsilon_a})^{-1} & \text{for exchange,} \end{cases}$$

and

$$V_a = (12.5\ \mathrm{MeV}) \cdot A_a.$$

The quantity $K_{\alpha,p}$ is given by Eq. (16); the final state density ω_{NT} is given by Eq. (12); and X_{NT} is given by Eq. (17). The finite well depth corrections in the state densities of (12) are made assuming a well depth of

$$V = \begin{cases} V_1(2Z/A) & \text{if } n_\pi = 0, \\ V_1 & \text{otherwise.} \end{cases}$$

A final change is that this model is now used for calculating nucleon exchange in nucleon and α particle inelastic scattering, whereas it was previously used only for d, t and ^{3}He scattering.

For the model describing inelastic and knockout processes with cluster degrees of freedom, only the overall normalization was changed. Thus, Eqs. (2)–(4) are still valid, but with a normalization constant of $C_a = 1/14$.

The model for excitation of collective states is unchanged, though there is evidence that the degree of forward peaking of the angular distributions for complex particle scattering will need to be increased relative to the main angular distribution systematics. Such an increase is not needed for nucleon scattering. An increase in the cross section normalization for complex projectiles of about a factor of 1.5 is also possible but has not been implemented.

Finally, work [43] on a comprehensive database, including much of the present database, indicates that isospin is conserved in the preequilibrium phase of a reaction when $E < 4E_{\mathrm{sym}}$. This assumption is made in the calculations discussed below.

B. Discussion of extra pair excitation

One of the more important changes made in this work is to allow the excitation of additional particle-hole pairs during direct nucleon transfer. This seems to be needed in both stripping and pickup. While the phenomenology does not tell us the physical picture underlying this observation, it is interesting to speculate on what it might be.

1. Secondary emission?

First, it seems unlikely that the extra cross section produced by this mechanism is due to pair excitation and secondary particle emission after the initial transfer. For primary nucleon emission, the cross section from direct transfer (stripping or exchange) is already made available to secondary preequilibrium emission in the exciton model, and while this yields a substantial increase in the secondary nucleon preequilibrium components, the contribution to the overall nucleon spectra is small. The biggest effect is for the (α, xp) spectra at 140 MeV, particularly for the lighter targets where an enhancement of 20–25% in the cross section in the middle of the spectrum was observed. However, even this large an effect occurs only when extra pair excitation is allowed in the direct stripping. Eliminating extra pair excitation (in the hope of accounting for it in this new way) would drastically decrease the stripping component in the middle of the spectrum, the region that contributes heavily to the secondary emission. For (d, p) stripping, even at 70–80 MeV and even with extra pair excitation included, the changes in the total spectrum due to secondary emission following the direct transfer are at most a few percent.

This mechanism should be even less important following direct pickup. Pickup leaves hole degrees of freedom, so that even though additional particle-hole pairs can be excited, the emission probabilities will be much lower than for states with the same number of excitons and excitation energy formed by stripping. Further, the relative yields of the different particle types that are currently described by the extra pair excitation seem to be directly correlated to the number and kind of nucleons transferred in the main direct reaction; this finding would not necessarily be expected if the extra cross section were due to secondary emission following direct transfer. Thus, it seems more likely that the extra cross section is due to primary emission that is closely related to the normal direct nucleon transfer. Several explanations seem possible.

2. Configuration mixing?

One explanation is configuration mixing. Here, the simple states that would normally be populated in direct nucleon transfer are assumed to be mixed with more complex states, enabling the configurations with extra particle-hole pairs to be populated. This is somewhat related to the first explanation. The particle-hole states which are normally considered in preequilibrium calculations are not eigenstates of the system, and it is the residual interactions not included in the generation of those states that cause the system to progress toward equilibrium. This equilibration process can then be looked

at either as a function of time or from a configuration mixing perspective. The difference here is that we are considering states in the residual nucleus, not the intermediate nucleus.

One of the fundamental assumptions in the exciton model, however, is that you do not reach the more complex configurations without passing through the simple doorway states, with the reaction then progressing through states of gradually increasing complexity. In the same way here, the coupling between the entrance channel and the mixed configurations would seem to have to occur through the simple states normally considered. But in the case of pickup, the deep hole states often do not exist, or at least their wavefunctions do not extend to the nuclear surface where the interaction is occurring.

3. Nucleon exchange?

Is it possible that the extra pairs are excited by nucleon exchange interactions accompanying the main transfer? This is an attractive possibility but appears unlikely. Comparing the value of X_{NT} with the extra factors in Eq. (19) that would be introduced for each new particle exchange shows that while they are sometimes of the same order of magnitude and have roughly the same dependence on target mass, their dependencies on the incident energy and projectile mass number are quite different and work in opposite directions.

4. Inelastic excitations?

Finally, we have the picture of inelastic excitations accompanying the nucleon transfer. A simultaneous excitation is most in keeping with a direct reaction (single interaction) picture and with the dependence of X_{NT} on the number and kind of transferred nucleons. This would imply that each transferred nucleon has some probability of exciting one or more particle-hole pairs during the transfer process. On the other hand, the reason for the form of the factor in Eq. (17) that depends on the transferred nucleons is certainly not clear.

In this picture, the inelastic excitation serves as a way of transferring extra energy to the product nucleus. This is especially crucial for pickup reactions when the deep hole states necessary to allow the emission of lower energy particles are not accessible. Of course, this physical picture gets to the same configurations as in the configuration mixing case, but it provides a more direct pathway to reach them.

VII. COMPARISONS WITH EXPERIMENT

With all of the changes described above—and most of them were made based on subsets of the data—a complete set of calculations for the spectra in the database was carried out. The results are encouraging. In comparing them with experiment, however, limitations in the calculations need to be remembered.

A. Practical considerations

First PRECO is a code designed primarily to study preequilibrium reactions, and the emphasis is on the first particle emitted. Equilibrium emission is considered only in the simple Weisskopf-Ewing evaporation model, not in the full angular-momentum-dependent Hauser-Feshbach model. Secondary particle emission (both preequilibrium and equilibrium) is only considered for nucleons and then only following primary nucleon emission. Secondary preequilibrium emission is allowed following primary emission in either the exciton model or the nucleon transfer model. Secondary evaporation is allowed following any primary nucleon emission—direct, preequilibrium, or equilibrium. At the higher incident energies considered here, secondary evaporation of complex particles (especially α particles) and later chance evaporation of nucleons are likely to contribute to the measured evaporation peaks but are not calculated, so these peaks will frequently be underestimated. Tertiary preequilibrium emission, while occurring, should not make a significant contribution (see [2]).

Then there is the question of outgoing energies. When the data are given as a function of either the center-of-mass (c.m.) energy of the outgoing particle or the exit channel energy (the combined c.m. energies of the emitted particle and recoiling nucleus), the calculations are plotted against the same energy parameter, and the scale in the figures is labeled accordingly. When the data are given in the laboratory system, the calculations are shown as a function of the channel energy, as this has repeatedly been shown to have a good correspondence with the laboratory energy spectrum, better than would be the case if the c.m. energy of the emitted particle were used. In the case of data vs. laboratory energy and calculations vs. channel energy, the figures have an x axis that is simply labeled ε, with no subscript.

B. Components

Figure 8 shows comparisons between calculation and experiment for sample reactions with incident protons, deuterons, and α particles. The different direct reaction components, including a preliminary estimate of the direct breakup component for incident deuterons, are indicated by dashed lines. Breakup is not included in the summed calculated spectrum since it is not yet generated within PRECO. The inelastic channels all have a collective component that contributes mainly at the highest emission energies and shows the influence of individual states and resonances. The deuteron and α particle inelastic channels also have two other direct components: a larger one in which the projectile is assumed to retain its cluster identity and excite a particle-hole pair in the target, and a smaller exchange component calculated in the nucleon transfer model. Finally, the lowest intensity (p, α) component is from α knockout. All other direct components represent direct stripping or pickup.

In general, the exciton model components (shown as short-dash curves in Fig. 8) become less important as the mass numbers of both the incident and outgoing particles increase. This is due to the increased complexity of the first states from which emission can occur and also to the extra factor of the projectile mass number in the exciton model mean square matrix elements. For the (p, xp) and (d, xp) spectra, the component from secondary preequilibrium emission within

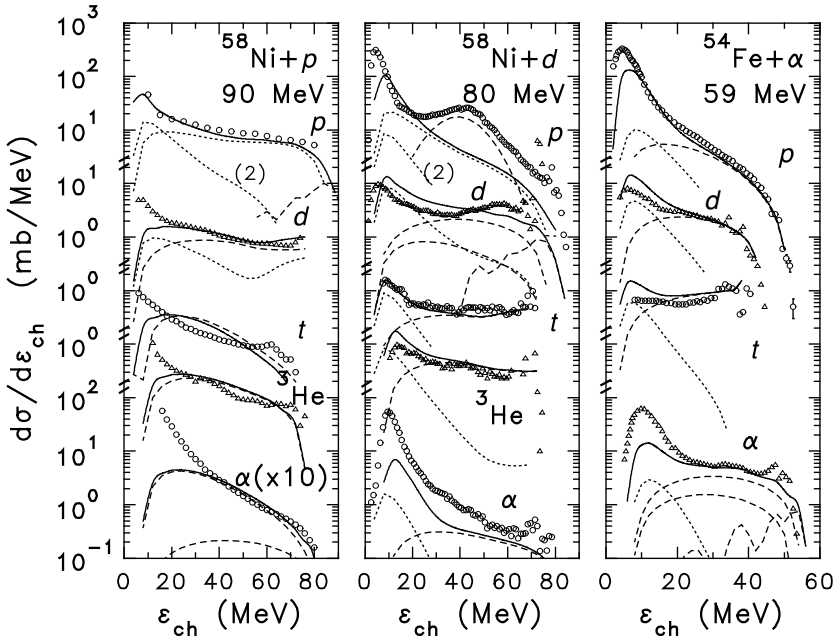

FIG. 8. Mechanisms contributing to the calculated spectra for sample reactions. The points show the data; the short-dash curves show the exciton model preequilibrium components; the long-dash curves give the supplementary direct reaction components described in the text; and the solid curves give the total calculated spectra excluding deuteron breakup. For the (p, xp) and (d, xp) spectra, both primary and secondary preequilibrium components are shown, with the secondary components labeled with the number 2.

the exciton model is also shown. Its contribution for incident α particles is too small to appear on the graph. Evaporation components are not shown in Fig. 8 but contribute to the cross sections represented by the solid curves.

C. Incident protons

Proton induced reactions were the first to be analyzed, and the results of sample comparisons with experiment are shown in Figs. 9–12. Bearing in mind the limitations of the calculations, the experimental spectra are well reproduced, in both magnitude and spectral shape. It is important to note in these and succeeding figures that the relative intensities of the different emitted particles vary by two orders of magnitude and that a single spectrum can show an intensity variation of up to three orders of magnitude for (p, α) [four for (α, p)].

There are, of course, some remaining problems. The calculations overestimate the α particle intensities for tin and gold at an incident energy of 29 MeV (see Fig. 9); they underestimate the triton intensity for aluminum at 62 MeV (see Fig. 11); and the shape of the calculated triton spectra at 90 MeV (see Fig. 12) looks too soft, probably indicating an overprediction of extra pair excitation. In some cases at 90 MeV, the region just above the evaporation peak in the complex particle spectra seems to be deficient in calculated

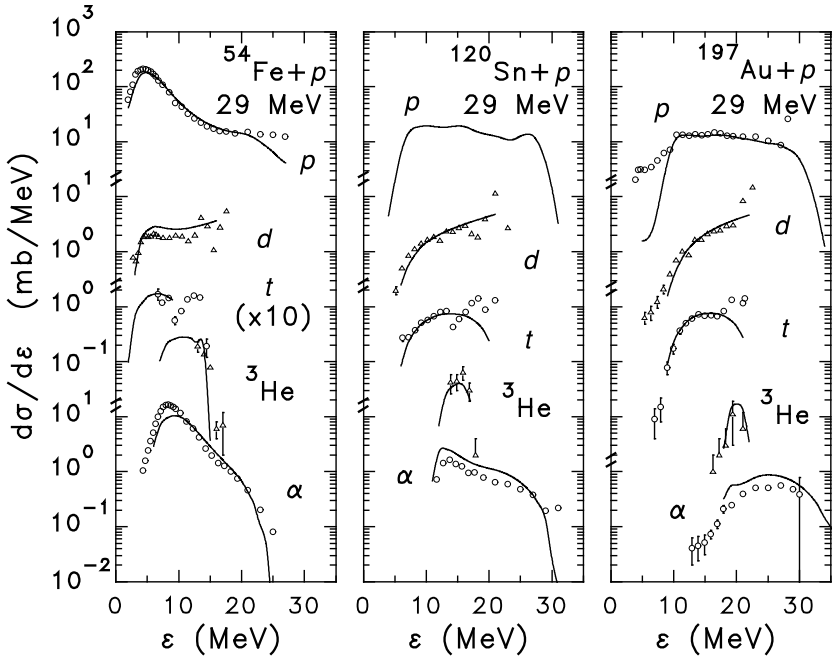

FIG. 9. Comparison between calculation and experiment for reactions induced by 29-MeV protons. The points show the data while the curves show the results from the current version of PRECO. There are no data for the ^{120}Sn(p, xp) reaction.

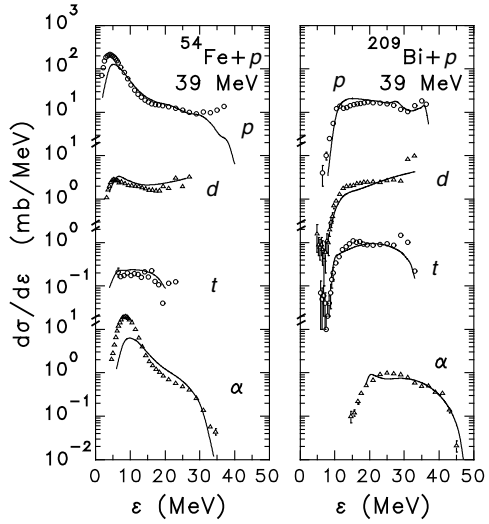

FIG. 10. Comparison between calculation and experiment for reactions induced by 39-MeV protons. The points and curves have the same significance as in Fig. 9.

cross section. Increasing the number of extra pairs that can be excited during direct pickup from three to four makes almost no change, and the exciton model components are quite small so that allowing multiple preequilibrium emissions in the calculations would not help. This will need to be revisited with calculations that include all the evaporation components for complex particles.

D. Incident neutrons

Similar comparisons are shown for neutron induced reactions at energies up to 63 MeV in Figs. 13–16. At 14–15 MeV (see Fig. 13), all the components of the calculated ^{93}Nb$(n, x\alpha)$ spectrum (pickup, exciton model, and evaporation) dramatically overestimate the data, but otherwise the results look remarkably good. At higher incident energies, there is a spread of 2–4 MeV in the experimental beam energy that causes a broadening and smoothing of the measured spectra. Calculations have been performed at the midpoint energy only. Earlier work [39] showed that this is adequate except at the highest emission energies. At 28–29 MeV (see Fig. 14), the most notable problem is that the calculated (n, xp) spectrum for ^{28}Si cuts off at too low an excitation energy. Part of that is due to the spread in the beam energy, but the larger effect is that there are states in the residual nucleus that can physically be populated but that are not being counted in the calculated state densities. A similar effect is seen in Figs. 15 and 16 for incident energies of 49–50 and 63 MeV, though it looks less severe because of the compressed energy scale.

This problem results from the Fermi level moving down during particle emission and is similar to the situation with direct nucleon transfer. Here, the first emission occurs from a $(p_\pi, h_\pi, p_\nu, h_\nu) = (1, 1, 1, 0)$ configuration and would generally produce a $(p_\pi, h_\pi, p_\nu, h_\nu) = (0, 1, 1, 0)$ residual configuration. If the proton hole in the composite nucleus happens to occupy the single particle state just below the Fermi level, there would no longer be a hole in the residual nucleus since the Fermi level has moved down on particle emission. The configuration would still be populated, but it would have $(p_\pi, h_\pi, p_\nu, h_\nu) = (0, 0, 1, 0)$. Adding these configurations removes much of the discrepancy. The consistent inclusion of such configurations is the subject of further study. It is most important for light targets and particularly those with large pairing and/or shell corrections in the final nucleus. In general, the energy requirement from the Pauli exclusion principle (and therefore the threshold energy) for these "extra" states will be lower than for the main configuration, thus allowing the calculated cross section to extend to higher emission energies.

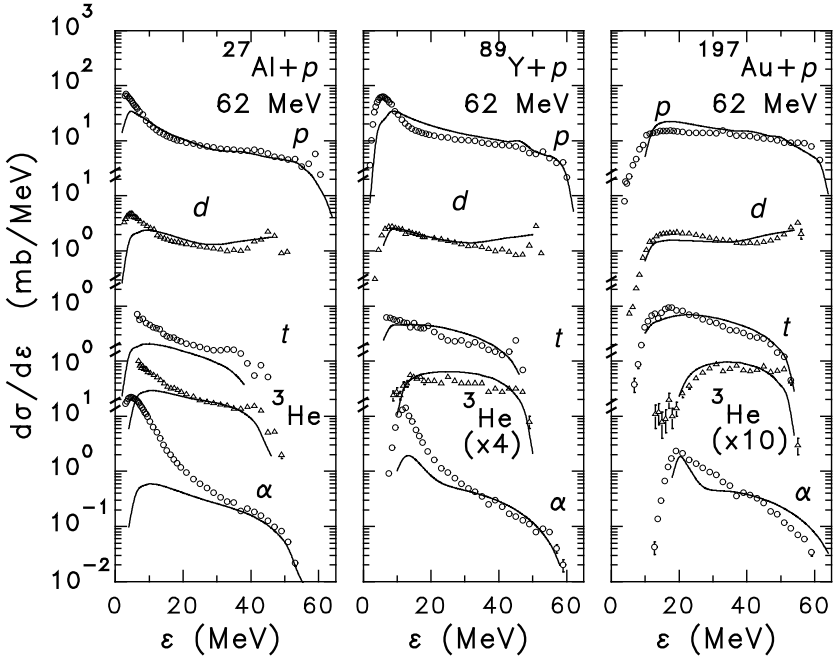

FIG. 11. Comparison between calculation and experiment for reactions induced by 62-MeV protons. The points and curves have the same significance as in Fig. 9.

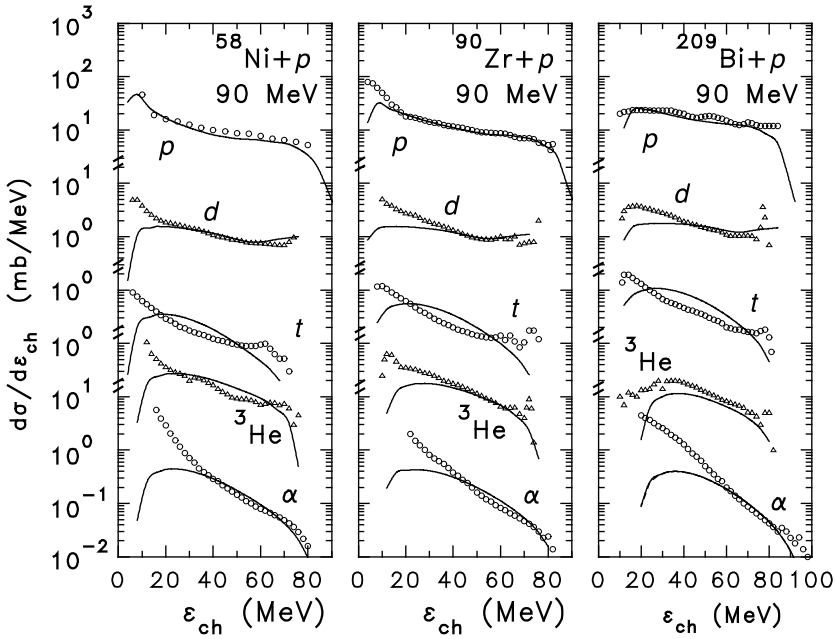

FIG. 12. Comparison between calculation and experiment for reactions induced by 90-MeV protons. The points and curves have the same significance as in Fig. 9.

Apart from that effect and the difficulty reproducing the evaporation peaks, the results generally look quite good. An obvious problem is that the ^{209}Bi$(n, x\alpha)$ evaporation peak at 63 MeV is significantly overestimated, rather than underestimated. The same behavior is noted in the ^{208}Pb$(d, x\alpha)$ reaction at 70 MeV discussed below. Since both reactions populate the same final nucleus, the problem may be related to the equilibrium shell corrections.

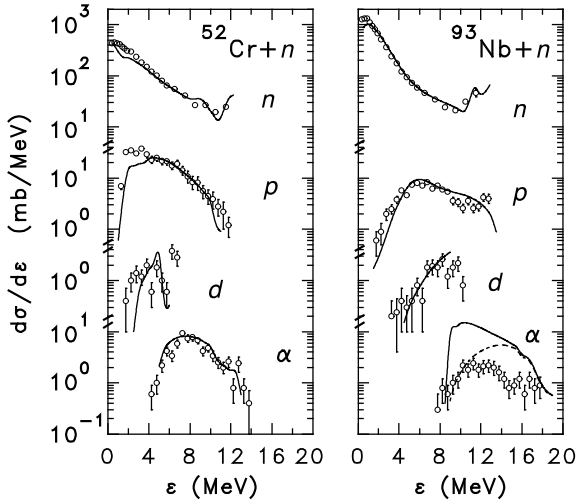

FIG. 13. Comparison between calculation and experiment for reactions induced by 14–15-MeV neutrons. The points and curves have the same significance as in Fig. 9. Here, the neutron spectra (data and calculations) are given as a function of the center-of-mass energy of the emitted neutron. Otherwise, the data are in the laboratory system and the calculations are plotted vs. the exit channel energy. The dashed curve for the ^{93}Nb$(p, x\alpha)$ reaction shows the direct pickup component.

E. Deuteron and ^{3}He induced reactions

Comparisons of deuteron and ^{3}He induced reactions are shown in Figs. 17 and 18. For incident deuterons, a rough breakup component is shown in the inclusive proton spectra, while the need for breakup components in the (^{3}He, xp) and (^{3}He, xd) calculated spectra in Fig. 17 is obvious. For ^{3}He breakup, the larger proton cross section suggests significant three-body breakup of the projectile.

As discussed above, the general level of agreement between calculation and experiment would be expected to improve if projectile breakup were properly included in PRECO. The cross section available to the exciton model calculations would correspondingly be reduced, making it possible to allow particle emission to occur from states formed by projectile dissociation prior to excitation of the first particle-hole pair. For incident deuterons of 70–80 MeV (see Fig. 18), there is

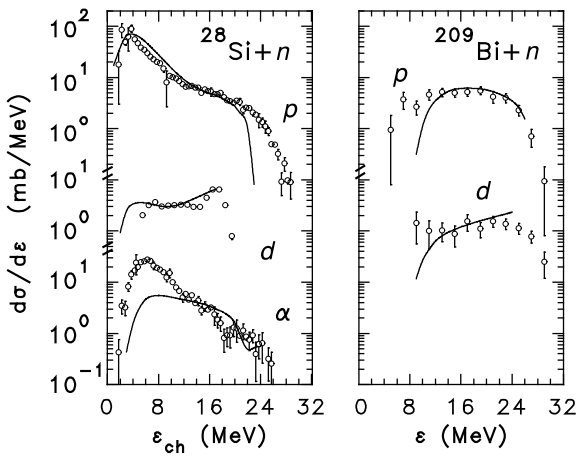

FIG. 14. Comparison between calculation and experiment for reactions induced by 28–29-MeV neutrons. The points and curves have the same significance as in Fig. 9.

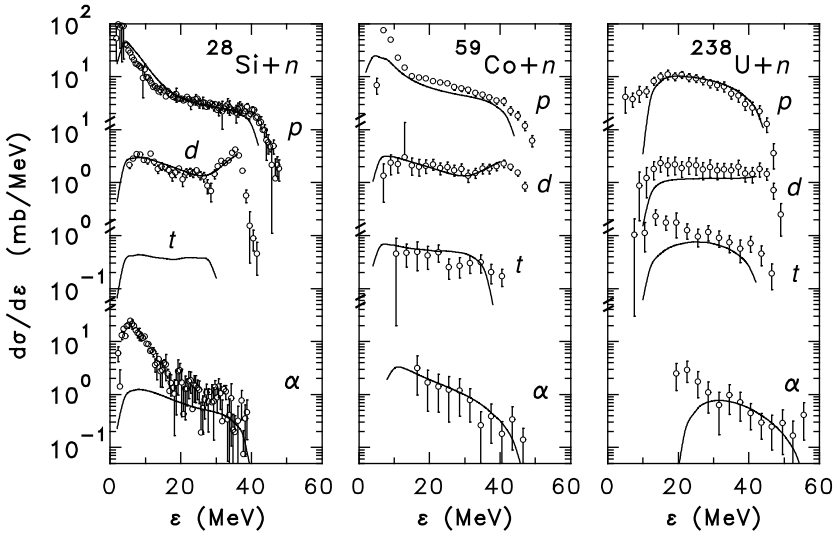

FIG. 15. Comparison between calculation and experiment for reactions induced by 49–50-MeV neutrons. The points and curves have the same significance as in Fig. 9. There are no triton data for ^{28}Si.

also an obvious problem in reproducing the α particle spectra. In addition, the shapes of the (d, xt) and $(d, x\alpha)$ spectra for the heavier targets are deficient in cross section at intermediate energies. The (d, xt) spectrum might be helped by eliminating the factor of $(2Z/A)$ reduction in V_1 used in the final state densities for pure neutron pickup. Another possibility would be a general increase in V_1 for heavy targets at the higher incident energies, such as was observed in neutron induced reactions. In that case, the change was thought to be related to the shift from a surface to a volume optical model potential [2].

F. Incident α particles

Figures 19–21 show comparisons for incident α particles. The agreement at 35–42 MeV (Fig. 19) and at 55–59 MeV (Fig. 20) is quite good, and there is little if any evidence in the angle-integrated spectra for a significant breakup component, even though evidence of a component at forward angles was noted at 59 MeV in angular distribution studies [44]. At 140 MeV, well above the energy range in which the exciton model has been benchmarked (though not above the energy/nucleon range), the agreement in spectral shape between calculation and experiment is not as good for triton, ^{3}He, and α emission. The calculated spectra are deficient in high energy particles where the calculations are dominated by nucleon transfer and, for α emission, by cluster scattering. The proton spectra show possible evidence of a significant breakup peak, and there is evidence for projectile breakup in the angular distributions. Clearly, much more work is needed at these higher incident energies.

VIII. SUMMARY AND CONCLUSIONS

Using a vastly expanded database, this work has succeeded in substantially improving the description of direct and preequilibrium continuum energy spectra for reactions with complex particles in the entrance and/or exit channel. The exciton model calculations are supplemented with a simple

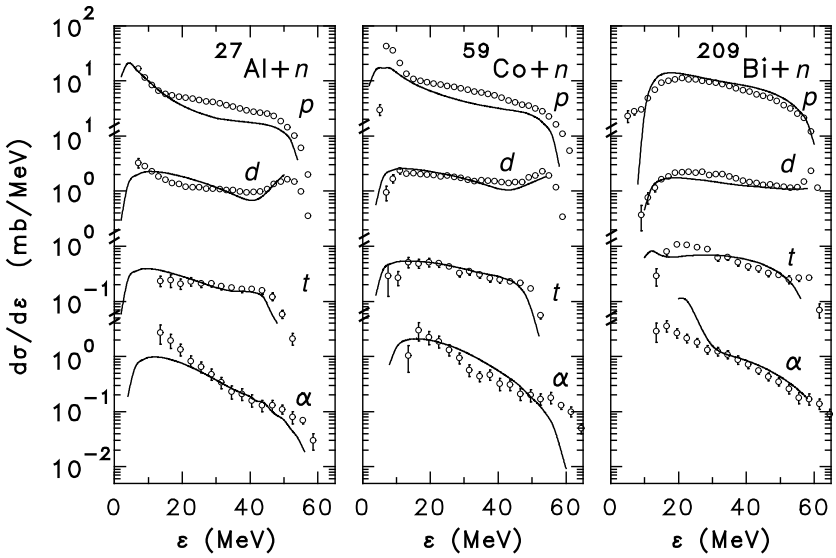

FIG. 16. Comparison between calculation and experiment for reactions induced by 63-MeV neutrons. The points and curves have the same significance as in Fig. 9.

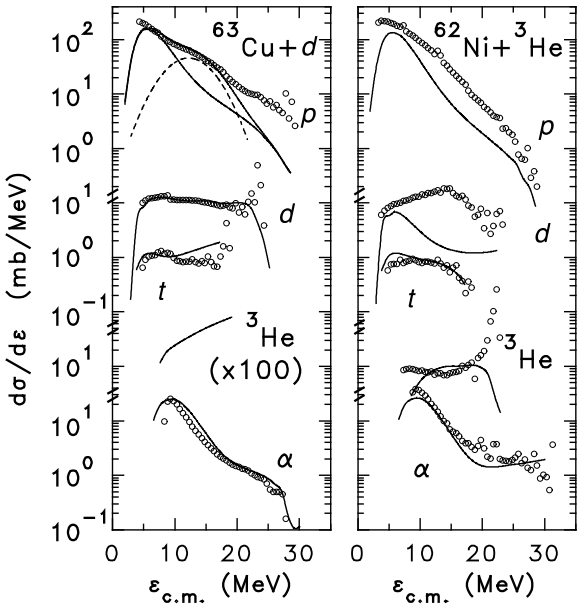

FIG. 17. Comparison between calculation and experiment for reactions induced by 24.7-MeV deuterons and 24.3-MeV ^{3}He. The points and curves have the same significance as in Fig. 9. The dashed curve shows a preliminary estimate of the deuteron breakup component. There are no (d, x ^{3}He) data.

collective excitation model and with phenomenological direct reaction models for direct nucleon transfer and reactions involving clusters. Much of the work here went into revising the model for direct nucleon transfer (stripping, pickup, and exchange). Evidence was found that the excitation of one or more particle-hole pairs sometimes occurs during nucleon transfer and that there is a difference in the overall normalization for the three types of transfer reactions. In addition, the normalization of the cluster model components was altered, and a projectile dependence was introduced in the exciton model mean square residual matrix elements. Information on the surface localization of the first interaction was also obtained. Section VI A gives the resulting model descriptions. What is not readily apparent, however, are the improvements in the state densities occurring in those equations relative to those used when the direct reaction models were first developed. These improvements are the result of previous work on the exciton model dealing with the inclusion of shell structure, pairing, and isospin effects.

A. Current status

The current description of nucleon induced reactions is both physically reasonable and fairly robust in its ability to describe a wide variety of experimental data up to incident energies of 90 MeV. Some question remains about the exact behavior of the average well depth at the point of the first interaction at the higher incident energies, and Koning and Duijvestijn [2] have suggested that guidance can be obtained from the relative sizes of the volume and surface imaginary terms of the optical potential. This suggests a gradual transition to a central or volume interaction. On the other hand, this work was encouraging in that the complex particle spectra for neutron induced reactions provided at least qualitative confirmation of the trends previously seen [39] in the (n, xp) spectra with regard to the finite well depth at the point of the initial interaction. In addition, Ref. [2] suggested that at energies of 90 MeV and above, the energy dependence of the exciton model mean square matrix element changes and the matrix elements approach a minimum asymptotic value. Both of these areas may well need further refinement in PRECO's exciton model and might affect the complex particle channels

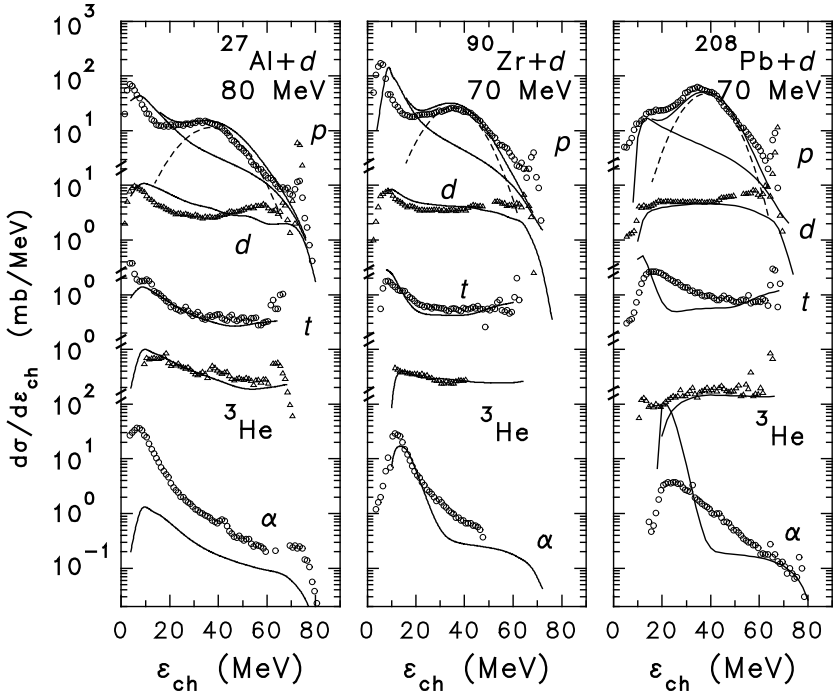

FIG. 18. Comparison between calculation and experiment for reactions induced by 70–80-MeV deuterons. The points and curves have the same significance as in Fig. 9. The dashed curves show a preliminary estimate of the deuteron breakup component.

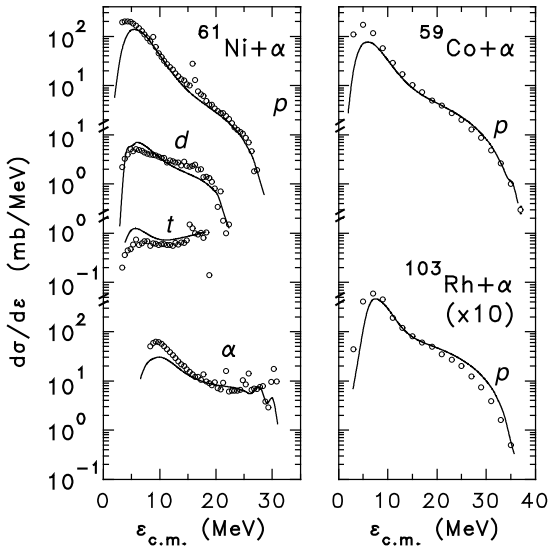

FIG. 19. Comparison between calculation and experiment for reactions induced by 35.5- and 42-MeV α particles. The points and curves have the same significance as in Fig. 9.

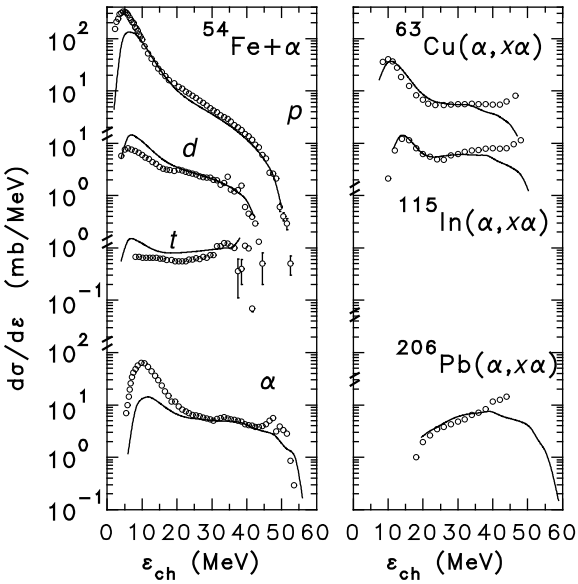

FIG. 20. Comparison between calculation and experiment for reactions induced by 58.8- and 54.8-MeV α particles. The points and curves have the same significance as in Fig. 9.

as well, but the current description is clearly adequate for many applications.

The results for complex projectiles are more tentative and contain points that lack a physical basis. In a practical sense, they are useful in estimating the energy spectra of emitted particles, but far more work and far more data are needed to adequately answer open questions.

B. Open questions

First, there is the need to develop and include a suitable description of projectile breakup reactions in which at least one projectile fragment is emitted strongly peaked in the forward direction with approximately the projectile velocity. Any absorbed fragment would then be allowed to initiate an exciton model calculation for secondary emission, and the cross section available to the main exciton model calculations would be reduced by the amount of the breakup cross section, just as it is currently reduced for the other direct reactions.

With these changes, it will most likely be advantageous to allow particle emission to begin from the $(p, h) = (A_a, 0)$ states rather than the states formed by the first particle-hole pair excitation. This effectively assumes that the projectile dissociates in the nuclear potential, prior to the first pair excitation. An open question is whether this initial configuration is appropriate for α particles at the lower incident energies

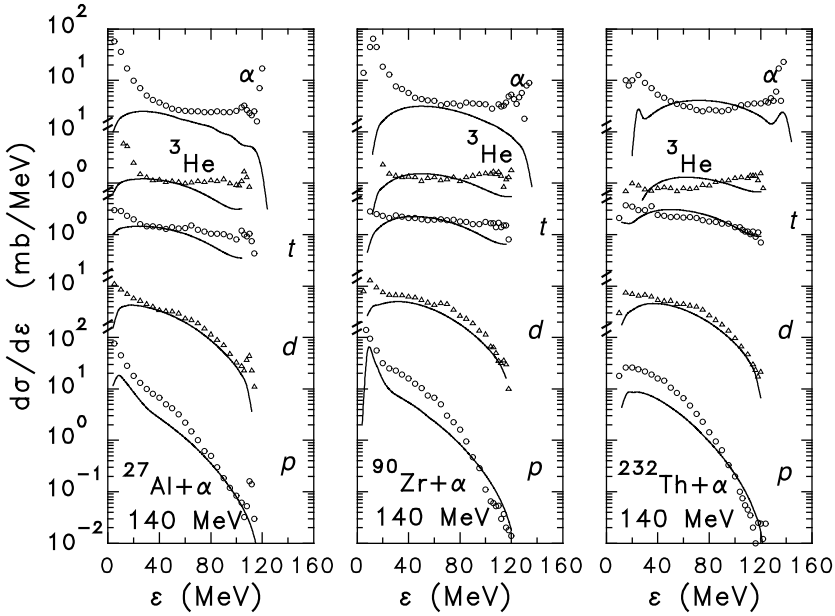

FIG. 21. Comparison between calculation and experiment for reactions induced by 140-MeV α particles. The points and curves have the same significance as in Fig. 9.

where the tight internal binding of the projectile makes breakup far less important. It is possible that some blend of the $(A_a, 0)$ and $(A_a + 1, 1)$ initial configurations—a blend that varies with the relative sizes of the incident energy and the projectile's internal binding—will be indicated. In studying these trends, it would obviously be desirable to have a significant body of α particle induced reaction data at incident energies in the gap between 60 and 140 MeV, and more complete data on a wide range of targets at lower energies. Data are also needed for deuteron induced reactions between 30 and 70 MeV and for ^{3}He induced reactions above 25 MeV.

Another, somewhat related, problem alluded to in the text is the assumption that deuteron and ^{3}He clusters can survive the excitation of a particle-hole pair in the target and then be reemitted. This is somewhat at odds with the dominance of the breakup peaks in the nucleon spectra. On physical grounds, one might expect that in the inelastic channels for loosely bound projectiles, exchange processes should be more important and cluster scattering with pair creation less important than is currently assumed. At the moment, the exchange normalization is largely determined by the one (^{3}He, xt) spectrum available, supplemented by evidence from the 140-MeV (α, $x\alpha$) spectra. Again, the needed new data mentioned above and particularly new results for (^{3}He, xt) on a variety of target nuclides at a variety of incident energies will be important in resolving this question. As with the initial configuration in the exciton model, it would seem to make sense to consider a cluster mechanism normalization that depends on the relative sizes of the incident energy and the projectile's internal binding energy.

C. Conclusion

In spite of remaining uncertainties, particularly with regard to complex particle induced reactions, this work has provided useful physical insights into the reaction mechanisms for preequilibrium reactions with complex particle channels and has produced a workable phenomenology. Information complementary to that from (N, xN) reactions has been obtained with regard to the surface localization of the initial interaction. Because of the breadth of the database used, this phenomenology permits the reasonable prediction of unmeasured or unmeasurable energy spectra from a wide variety of reactions.

ACKNOWLEDGMENTS

Special thanks go to Arjan Koning and the experimental team of Prof. Jean-Pierre Meulders for providing tables of the Louvain results, sometimes before they were formally published, and to Robert Haight for providing the LANSCE results in tabular form. The author is also grateful to Arjan Koning for helpful discussions. This work was performed at the Triangle Universities Nuclear Laboratory under U. S. Department of Energy Grant No. DE-FG02-97ER41033.

[1] J. J. Griffin, Phys. Rev. Lett. **17**, 478 (1966).
[2] A. J. Koning and M. C. Duijvestijn, Nucl. Phys. **A744**, 15 (2004).
[3] M. B. Chadwick, P. G. Young, D. C. George, and Y. Watanabe, Phys. Rev. C **50**, 996 (1994).
[4] A. J. Koning and M. B. Chadwick, Phys. Rev. C **56**, 970 (1997).
[5] P. Hodgson and E. Běták, Phys. Rep. **374**, 1 (2003).
[6] J. Dobeš and E. Běták, in *Proceedings of the International Conference on Reaction Models, Balatonfüred, 1977*, edited by L. P. Csernai (Budapest, 1977), p. 195, as cited on p. 23 of Ref. [5].
[7] A. Iwamoto and K. Harada, Phys. Rev. C **26**, 1821 (1982).
[8] J. Bisplinghoff, Phys. Rev. C **50**, 1611 (1994).
[9] C. Kalbach, Phys. Rev. C **19**, 1547 (1979).
[10] C. Kalbach, J. Phys. G: Nucl. Part. Phys. **21**, 1519 (1995).
[11] C. Kalbach, Acta Phys. Slov. **45**, 685 (1995).
[12] C. Kalbach, J. Phys. G: Nucl. Part. Phys. **24**, 847 (1998).
[13] C. Kalbach, Phys. Rev. C **62**, 044608 (2000).
[14] C. K. Walker, Triangle Universities Nuclear Laboratory Report "Users Manual for PRECO-2000: Exciton Model Preequilibrium Code with Direct Reactions," 2001 (unpublished), available from the code distribution center at the National Nuclear Data Center (Brookhaven National Laboratory) and through the Radiation Safety Information Computing Center (Oak Ridge National Laboratory).
[15] C. Kalbach, J. Phys. G: Nucl. Part. Phys. **25**, 75 (1999).
[16] C. Kalbach, Z. Phys. A **283**, 401 (1977).
[17] C. Kalbach, "PRECO-D2: Program for Calculating Preequilibrium and Direct Reaction Double Differential Cross Sections," Los Alamos National Laboratory Report LA-10248-MS, 1985 (unpublished).
[18] C. Kalbach, J. Phys. G: Nucl. Part. Phys. **21**, 1499 (1995).
[19] R. Bonetti and L. Milazzo-Colli, Phys. Lett. **B49**, 17 (1074).
[20] H. Kalka, M. Torjman, and D. Seeliger, Phys. Rev. C **40**, 1619 (1989).
[21] F. E. Bertrand and R. W. Peelle, Phys. Rev. C **8**, 1045 (1973).
[22] F. E. Bertrand, R. W. Peelle, and C. Kalbach-Cline, Phys. Rev. C **10**, 1028 (1974).
[23] S. M. Grimes, R. C. Haight, and J. D. Anderson, Nucl. Sci. Eng. **62**, 187 (1977).
[24] S. M. Grimes, R. C. Haight, and J. D. Anderson, Phys. Rev. C **17**, 508 (1978).
[25] S. M. Grimes, R. C. Haight, K. R. Alvar, H. H. Barschall, and R. R. Borchers, Phys. Rev. C **19**, 2127 (1979).
[26] J. Bisplinghoff, J. Ernst, R. Lohr, T. Mayer-Cuckuk, and P. Meyer, Nucl. Phys. **A269**, 147 (1976).
[27] R. W. West, Phys. Rev. **141**, 1033 (1966).
[28] A. Chavarier, N. Chevarier, A. Demeyer, G. Hollinger, P. Pertosa, and T. M. Duc, Phys. Rev. C **11**, 886 (1975).
[29] J. R. Wu, C. C. Chang, and H. D. Holmgren, Phys. Rev. C **19**, 698 (1979).

[30] F. B. Bateman, R. C. Haight, M. B. Chadwick, S. M. Sterbenz, S. M. Grimes, and H. Vonach, Phys. Rev. C **60**, 064609 (1999), and data tables supplied by the authors.
[31] J. R. Wu, C. C. Chang, and H. D. Holmgren, Phys. Rev. C **19**, 659 (1979).
[32] J. R. Wu, C. C. Chang, and H. D. Holmgren, Phys. Rev. C **19**, 370 (1979).
[33] A. Chevarier, N. Chevarier, A. Demeyer, A. Alevra, I. R. Lukas, M. T. Magda, and M. E. Nistor, Nucl. Phys. **A237**, 354 (1975).
[34] S. Benck, I. Slypen, J. P. Meulders, and V. Corcalciuc, At. Data Nucl. Data Tables **78**, 161 (2001), and data tables supplied by the authors.
[35] S. Benck, I. Slypen, J. P. Meulders, and V. Corcalciuc, Nucl. Sci. Eng. **141**, 55 (2002), and data tables supplied by the authors.
[36] N. Nica, S. Benck, E. Raeymackers, I. Slypen, J. P. Meulders, and V. Corcalciuc, J. Phys. G: Nucl. Part. Phys. **28**, 2823 (2002), and data tables supplied by the authors.
[37] E. Raeymackers, S. Benck, N. Nica, I. Slypen, J. P. Meulders, V. Corcalciuc, and A. J. Koning, Nucl. Phys. **A726**, 175 (2003), and data tables supplied by the authors.
[38] E. Raeymackers, S. Benck, I. Slypen, J. P. Meulders, N. Nica, V. Corcalciuc, and A. J. Koning, Phys. Rev. C **68**, 24604 (2003), and data tables supplied by the authors.
[39] C. Kalbach, Phys. Rev. C **69**, 014605-1 (2004).
[40] A. Pavlik and H. Vonach, "Evaluation of the angle integrated neutron emission cross sections from the interaction of 14 MeV neutrons with medium and heavy nuclei," Fachinformations-Zentrum Karlsruhe Report 13-4, 1988 (unpublished).
[41] A. M. Kalend, B. D. Anderson, A. R. Baldwin, R. Madey, J. W. Watson, C. C. Chang, H. D. Holmgren, R. W. Koontz, J. R. Wu, and H. Machner, Phys. Rev. C **28**, 105 (1983).
[42] C. Kalbach, Phys. Rev. C **69**, 014605 (2004).
[43] C. Kalbach, *Isospin Conservation in Preequilibrium Reactions* (in preparation).
[44] C. Kalbach, Phys. Rev. C **37**, 2350 (1988).
[45] C. Kalbach, Nucl. Sci. Eng. **115**, 43 (1993).
[46] A. Takahashi, M. Gotoh, Y. Sasaki, and H. Sugimoto, "Double and Single Differential Neutron Emission Cross Sections at 14.1 Mev: Vol. 2," OKTAVIAN Report A-92-01, Osaka University, Department of Nuclear Engineering, 1992 (unpublished).
[47] G. Duhamel, L. Marcus, H. Langevin-Joliot, J. P. Didlez, P. Narboni, and C. Stephan, Nucl. Phys. **A174**, 485 (1971).
[48] G. Bruge, A. Chaumeaux, R. DeFries, and G. C. Morrison, Phys. Rev. Lett. **29**, 295 (1972).
[49] F. G. Perey in *Nuclear Spin and Parity Assignments*, edited by N. B. Gove (Academic, New York, 1966), taken from A. DeShalit and H. Feshbach, *Theoretical Nuclear Physics* (Wiley, New York, 1974), p. 79.
[50] C. M. Perey and F. G. Perey, Phys. Rev. **132**, 735 (1963).
[51] E. R. Flynn, D. D. Armstrong, J. G. Beery, and A. G. Blain, Phys. Rev. **182**, 113 (1969).
[52] P. P. Urone, L. W. Put, H. H. Chang, and B. W. Ridley, Nucl. Phys. **A163**, 225 (1971).
[53] L. McFadden and G. R. Satchler, Nucl. Phys. **84**, 177 (1966).
[54] A. E. Glassgold, *Progress in Nuclear Physics* (Pergamon, London, 1959) Vol. 7, taken from B. G. Harvey, *Introduction to Nuclear Physics and Chemistry*, p. 188 (Prentice-Hall, Englewood Cliffs, NJ, 1962).